جامعة أبو بكر بلقايد
UNIVERSITÉ DE TLEMCEN

Pan African University
Institute of Water and Energy Sciences

PAN AFRICAN UNIVERSITY

Institute of Water and Energy Sciences (Incl. Climate Change)

DESIGN AND CHARACTERIZATION OF ORGANIC SOLAR CELLS BASED ON NON-FULLERENE ACCEPTORS.

Ogechi Vivian Nwadiaru

Date: 05/09/2017

Master in ***Energy, Engineering track***

President: Prof. Youm Issakha

Supervisor: Dr. Harald Hoppe

External Examiner: Dr. Sofiane Amara

Internal Examiner: Dr. Abdellah Benyoucef

Academic Year: 2016-2017

DECLARATION

I Nwadiaru Ogechi Vivian, hereby declare that this thesis represents my personal work, realized to the best of my knowledge. I also declare that all information, material and results from other works presented here, have been fully cited and referenced in accordance with the academic rules and ethics.

Student
Ogechi Vivian Nwadiaru

Signature…….……. Date: August 29, 2017

DEDICATION

To my loving parents and children all over the world who have to study in poor lighting conditions.

ACKNOWLEDGEMENT

This work would not be possible if I did not exist in this space and time, as such I am forever grateful to God who made my existence possible and to my parents through whom this was achieved. I would also like to express my gratitude to the initiators and implementers of the Pan African University, who have made it their task to ensure that higher learning in Africa is revolutionized.

The practical work done is this thesis was made possible through the close mentorship of Prof. Daniel Egbe who through the work of ANSOLE, was able to connect me to the working group of AG. Hoppe at the Center of Energy and Environmental Chemistry (CEEC) Jena for this research. I am also very grateful to Dr. Harald Hoppe, for the several hours of work, his astounding knowledge in the field of materials science he devoted to ensuring that a decent master thesis was made possible and also for accepting to host me in his working group for this research.

My colleagues at CEEC were such a wonderful set of people and their various inputs cannot be left unrecognized; Shahidul Alam for his very patient explanations of several laboratory procedures and for using his expertise for the fabrication of the cells, Rico for his very intelligent inputs and for supervising my internship, Anne and Cyril for their constant support for this I am sincerely grateful.

I would also like to acknowledge the support of my dear colleagues at PAUWES Tonny, Diana, Eva and my best friend Ogechi Anya who have provided me the adequate academic and psychological stronghold required to complete this thesis.

I am also grateful to the director of PAUWES Prof. Zerga and my former supervisor Dr. Yacine Kouhlane for steering my paths towards this interesting field of Energy materials. To all the many people whose names have been left out, I wish to extend my gratitude to you, because your words of encouragement made it possible to get to this point, I appreciate your support and kindness.

ABSTRACT

The rise in the global population is constantly putting pressure on the available energy resources leading to an excessive exploitation of conventional energy resources such as fossil fuels. The use of fossil fuels has led to several health challenges and environmental issues, this has therefore informed the decision to switch to renewable energy resources. Solar PV technology has carved a niche for itself as a low cost option for providing electricity even to the most inaccessible areas, however convention technologies are relatively limited in their application due to their rigid nature and difficult manufacturing steps. This has created an opportunity for research into materials that can be easily fabricated and used for their photovoltaic effect, hence the recent interest in the field of organic photovoltaics. Organic photovoltaic research has gained momentum since the discovery of conducting polymers and holds a promise for a low cost alternative to conventional PV technologies for providing access to electricity. The challenge currently facing the commercialization of this technology is the very modest efficiencies and lifetimes currently achieved. An improvement in the performance of these devices can be made possible by ensuring proper energy level alignment and matching of donor-acceptor materials that have a wide absorption in the visible range.

In this work, AnE-PVstat was investigated for its compatibility with novel acceptor materials, PCE of 0.88 % was obtained with ITIC as against 1.89 % with PCBM the reference sample without a solvent additive. It is also important to note the high Voc of about 1 V obtained with these electron acceptors which is possibly linked to alignment of the HOMO level of the polymer and the LUMO level of the acceptors. It was also discovered that upon utilization of a solvent additive the PCE of devices based on ITIC increased to 0.88% while those for PCBM increased to 2.2 %. This increase in PCE obtained from the use of solvent additive is a critical one as it serves as an indication of the possibility of refining the morphology of the active layer without including an additional annealing step, thereby increasing the efficiency of the roll to roll process for commercialization. The thesis further demonstrated that an electronic compatibility is not sufficient for achieving high performance in solar cell devices but also a morphological compatibility is required.

Key words: Organic Photovoltaics, PCE, Morphology, Energy level alignment

RESUME

L'augmentation de la population mondiale exerce une pression constante sur les ressources énergétiques disponibles, ce qui entraîne une exploitation excessive des ressources énergétiques conventionnelles telles que les combustibles fossiles. L'utilisation des combustibles fossiles a entraîné plusieurs problèmes de santé et des problèmes environnementaux, ce qui a donc permis de passer aux ressources énergétiques renouvelables. La technologie photovoltaïque solaire s'est sculpté une place comme une option à faible coût pour fournir de l'électricité même aux zones les plus inaccessibles. Cependant les technologies conventionnelles sont relativement limitées dans leur application en raison de leur nature rigide et les difficultés associées aux étapes de leur fabrication. Cela a créé une opportunité pour la recherche de matériaux qui peuvent être facilement fabriqués et utilisés pour leur effet photovoltaïque, d'où l'intérêt récent dans le domaine du photovoltaïque organique. La recherche en matière de photovoltaïque organique a pris de l'ampleur depuis la découverte des polymères conducteurs et détient la promesse d'une alternative peu coûteuse aux technologies photovoltaïques classiques pour l'accès à l'électricité. Le défi qui se pose actuellement à la commercialisation de cette technologie est l'efficacité et les durées de vie très modestes actuellement atteintes. Une amélioration de la performance de ces dispositifs peut être rendue possible en garantissant un alignement correct du niveau d'énergie et l'adaptation des matériaux donneurs-accepteurs qui ont une large absorption dans la gamme visible. Dans ce travail, AnE-PVstat a été étudié pour sa compatibilité avec de nouveaux matériaux accepteurs. PCE de 0,88% a été obtenu avec ITIC contre 1,89% avec PCBM, l'échantillon de référence sans additif solvant. Il est également important de noter le Voc élevé d'environ 1 V obtenu avec ces accepteurs d'électrons qui est probablement lié à l'alignement du niveau HOMO du polymère et du niveau LUMO des accepteurs. On a également découvert qu'avec l'utilisation d'un additif solvant, le PCE des dispositifs basés sur l'ITIC se sont élevés à 0,88% alors que ceux pour PCBM à 2,2%. Cette augmentation de PCE obtenue à partir de l'utilisation d'un additif solvant est critique. Ceci parce qu'elle sert d'indication de la possibilité de raffiner la morphologie de la couche active sans inclure une étape de recuit supplémentaire, ce qui augmente l'efficacité du processus de roulement à rouleau pour la commercialisation. La thèse, de façon supplémentaire a démontré qu'une compatibilité électronique n'est pas suffisante pour atteindre des performances élevées dans les appareils à cellules solaires, mais aussi une compatibilité morphologique est nécessaire.

Mots clés: Photovoltaïque organique, PCE, morphologie, alignement de niveau d'énergie

Table of Contents

Acronyms

AFM – Atomic Force Microscopy

BHJ – Bulk heterojunction

CdTe – Cadmium Telluride

CIGS – Copper Indium gallium selenide

CSP - Concentrated solar power

CV- Cyclic Voltammetry

D-A – Donor - acceptor

DSSC – Dye – Sensitized Solar Cell

ETL – Electron Transfer Layer

EQE – External Quantum Efficiency

FF - Fill Factor

HOMO - Highest Occupied Molecular Orbital

HTL – Hole Transfer Layer

ISC - Intersystem crossing

ITO - indium tin oxide

L_D - Exciton diffusion length

LUMO - Lowest Unoccupied Molecular Orbital

MPP – Maximum Power Point

OHJ – Ordered Heterojunctions

OPV – Organic Photovoltaic

OSC – Organic Solar Cell

PCE - Power Conversion Efficiency

PEDOT:PSS - Poly(ethylenedioxythiophene): poly(styrenesulphonate)

PL- Photoluminescence

PV- Photovoltaic

P3HT – Poly(3-hexythiophene-2,5-diyl)

List of figures

List of Tables

1 INTRODUCTION

Energy is undoubtedly a basic human need as evident from our daily activities. It is required for activities ranging from simple household cooking or cleaning to the running of several manufacturing plants. As such with any increase in the use of sophisticated devices and population comes an increase in the demand for energy. As populations expand, living standards improve and consumption rises, total demand for energy is expected to increase by 21% by 2030 [1]. This drive in demand led to a zealous exploration of fossil fuels, the result of which are high emissions, global warming and several health related complications resulting from burning fossil fuels. The health impact has been linked to millions of cases of lost work hours in the United States of America and the rise in the number of respiratory and cardiovascular diseases by WHO [2, 3] Aside the environmental impact the price variability of fossil fuels affects energy security negatively in nations that are heavily dependent on fossil fuel for power supply. With these in mind great attention has been shifted to renewable clean energy sources. The current global need to balance the increasing energy demand with environmental sustainability and energy security necessitated a movement towards the utilization of renewable energy resources. This shift to more sustainable energy resources is also driven by the global adoption of the 17 sustainable development goals, of which goal 7 is to ensure access to affordable and clean energy [4].

The deployment of renewable energy technologies has seen remarkable growth in recent decades, supported by enabling policies and steep cost reductions. However, there is still a lot of room for growth as the world in 2014, relied on renewable sources for around 13.8% of its total primary energy supply [5]. The decision on which technology to deploy is made based on specific resource availability, energy payback time, cost and demand profile of the location. In this light, solar energy technologies have been widely embraced based on the assumption that the rays of the sun get to most part of the earth unlike other renewable energy resources that are location specific such as wind, hydro and geothermal. Broadly speaking there are two ways in which the power of the sun can be harnessed; by direct

conversion to electricity through the utilization of the photovoltaic effect in solar cells and by utilizing the thermal energy which is then used for heating applications or electricity production with the use of solar concentrators.

Concentrated solar power (CSP) requires large scale investment and as such cannot be used on a household level to supply the electricity demand of very remote areas with low economic activities. Photovoltaic (PV) devices on the other hand have gained popularity with several remote applications such as in solar home systems, calculators, street lighting, solar lamps, solar water pumping and more. Their popularity can also be attributed to the fact that they offer fast and efficient direct conversion of sun light into electrical energy. Considering the wide gap between urban and rural energy access, it is only rational to turn to decentralized energy technologies like PV to provide electricity to single households in rural areas. This in turn will help spur up the electrification rates in Africa especially Sub-Saharan Africa where two-thirds of the population are currently living without electricity [6].

Conventional PV devices can serve as a competitive method for providing access to electricity in remote locations with modular costs as low as $0.3/W especially in solar rich Africa with a direct normal irradiation as shown in Figure 1.1, however the complexity of its manufacturing process, can cut back on the energy gain. This Creates room for further improvement in the costs of manufacturing of PV devices, also their rigidity limits their application as most of the conventional PV devices are not flexible. Furthermore, they also present a challenge on the end of life disposal, seeing as some of the materials used in their fabrication are toxic to the environment. Therefore, the task at hand is to fabricate devices that can ensure an efficient photo conversion process at low cost while maintaining its stability with little or no environmental impact in the course of its lifetime.

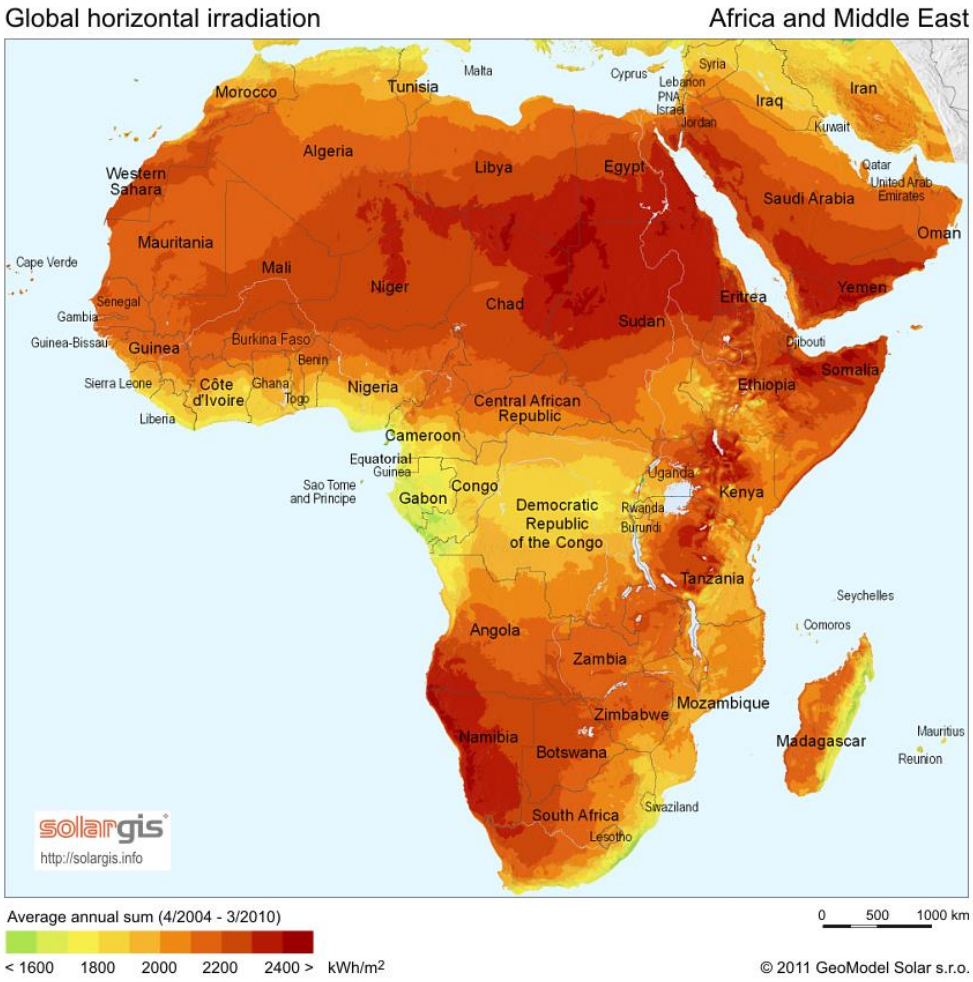

Figure 1.1: Map of Africa showing the daily solar Insolation

1.1 Photovoltaic Conversion Devices

According to a World Energy Assessment conducted in the year 2000 by the United Nation Development Programme, it was reported that the annual potential of solar energy was 1,575–49,837 exajoules (EJ) [7]. This is more than enough to cover the world final energy consumption which was reported by IEA as approximately 0.4 EJ in 2014 [8], making solar energy a reliable and sufficient source for ensuring equitable access to energy. Solar cells work through the fundamentals of the photovoltaic effect, the photovoltaic (PV) effect discovered by Becquerel in 1839 [9] is the basic physical process, by which the semiconductor material converts electromagnetic radiation (sun light) into electric power. The discovery formed the foundation for research into solar cells and it was only partly deployed for extra-terrestrial applications, in the 1960s photovoltaics received its major

support from the space industry for research and development as an alternative power source to the primary battery power source. This helped in increasing the time for different expeditions, when cells were added to the outside of the body of space crafts, with no major changes to the spacecraft or its power systems. Improvements in the efficiencies were for a long period driven by the space power market until the oil crisis in 1973 and the push by the National Science Foundation's program "Research Applied to National Needs" began to push for terrestrial application of solar cells. Today, it is a rapidly growing and increasingly important renewable alternative to conventional fossil fuel electricity generation, but compared to other electricity generating technologies like hydropower, it is still regarded as an emerging technology.

1.1.1 Properties of Sunlight

The everyday light visible to the human eye is only a fraction of the solar radiation incident on the surface of the earth. Sunlight is an electromagnetic radiation consisting of light characterized by different wavelengths as shown in Figure 1.2. The electromagnetic spectrum is made of all the different kinds of electromagnetic waves. Visible light, ultraviolet light, and infrared light make up a very small part of the electromagnetic spectrum.

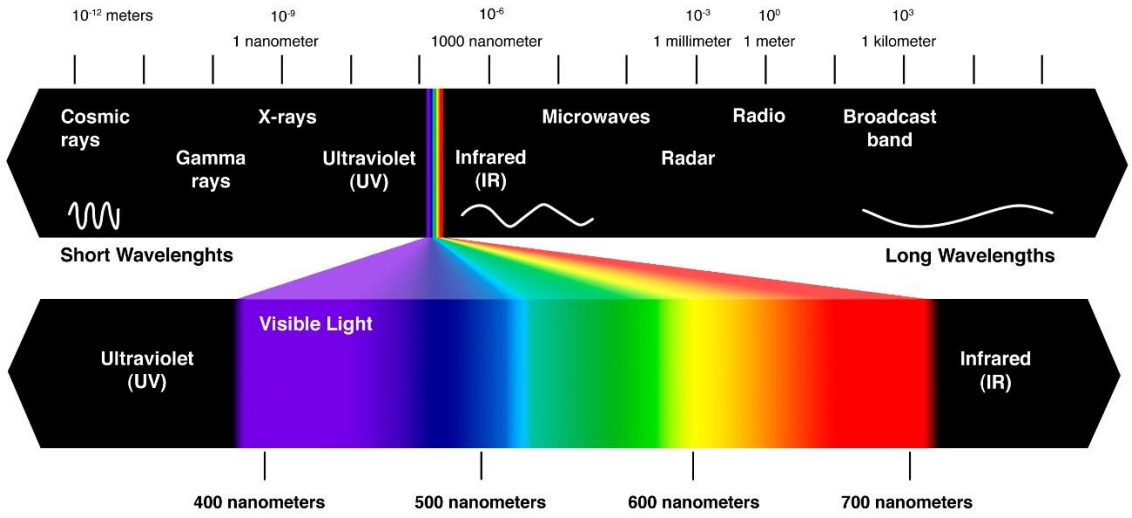

Figure 1.2 Electromagnetic spectrum of light [10]

Based on the works of Planck and Einstein, light may be viewed as consisting of "packets" or particles of energy, called photons. These photons are very important in the photovoltaic process as they determine the amount of energy available for the release of mobile charge carriers. This energy (E) is inversely related to the wavelength (λ) of the incident light as given in equation 1.1 and 1.2

$$E = \frac{hc}{\lambda} \tag{1.1}$$

$$E(eV) = \frac{1240}{\lambda(nm)} \tag{1.2}$$

Where, h (6.626×10^{-34} joule $\cdot$ s) is Planck's constant and c (2.998×10^{8} m/s) is the speed of light. This relationship implies that incoming radiation of high energy photons (such as "blue" light) has a short wavelength, while light consisting of low energy photons (such as "red" light) has a long wavelength. The fraction of sunlight that can be absorbed by each material varies depending on its chemical structure and this is important for any solar cell device fabrication. This is because, solar cells work on the principle of converting light to electricity, hence the absorption properties (Optical band gap and molecular energy levels) of the materials that make up the solar cell has an impact on its efficiency and performance. The absorption process in the visible light range is based on the principle of electronic transition in atoms or molecules upon absorbing suitable energy from an incident light that allows electrons to excite from a lower energy state to higher excited energy state. The mismatch of the polymer absorption spectra and the solar irradiance spectrum has been one of the reasons for low efficiencies of devices. In order to improve the performance and economics of solar cell devices different materials have been employed and are still being researched over time. These generations of evolution in the history of solar devices is discussed in the following section.

1.1.2 Solar cell Generations

Solar cell technologies have evolved overtime from energy intensive monocrystalline silicon solar cells to roll to roll solution processed organic solar cells. Hence, solar cells can be classified according to the point in time they started playing a big role in the solar cell field- into first, second and third generation cells [11].

The first-generation cells—also called conventional, traditional or wafer-based cells—are made of crystalline silicon, the commercially predominant PV technology, that includes materials such as polysilicon and monocrystalline silicon. About 90% of the commercially produced solar cells are based on this generation.

Second generation cells— the cells in this category are designed to address cost issues related to the manufacturing process as they are adapted to cheaper substrates like glass and the thin film could be done via vapour deposition. They include amorphous silicon, CdTe and CIGS cells and are commercially significant in utility-scale photovoltaic power stations, building integrated photovoltaics or in small stand-alone power system. Regardless of their prospect for providing cheaper devices, this generation of cells would also hit certain price limits per watt due to efficiency limits and the material costs.

The third generation of solar cells includes a number of thin-film technologies often described as emerging photovoltaics—most of them have not yet been commercially applied and are still in the research or development phase. In addition, the solar cells in this category utilizes completely new concepts in terms of device architectures and materials, common examples are Dye – Sensitized Solar Cells (DSSCs) [12] and Organic Solar Cells (OSCs). DSSCs are based on combination of dyes with metal oxides and electrolyte. The efficiencies of DSSC are in the range of 12 % for small lab scale devices, while the lifetime of the devices is rather low compared to inorganic solar cells. For OSCs efficiencies between 11 – 13 % have been achieved so far but also on a laboratory scale [13, 14]. Many of these devices use organic materials, often organometallic compounds as well as inorganic substances. Anthracene was the first organic compound in which photoconductivity had been observed by Pochettino in 1906 [15] and which started a new

era for studying organic compounds for electronic applications. Especially in the last decade the field of organic photovoltaics (OPVs) has been growing really fast and showing promising potential for rather cheap PV technology. Despite the fact that their efficiencies have been low and the stability of the absorber material was often too short for commercial applications, there is a lot of research invested into these technologies as they promise to achieve the goal of producing low-cost, high-efficiency solar cells [12, 16]. With this promise in mind the field of organic photovoltaics has garnered a lot of attention and has become a fascinating field of research in the development of affordable renewable energy technologies.

1.2 State of the Art of Organic Solar Cells

An organic cell is one that converts electromagnetic radiation to electricity, however the material used in the absorption of light is an organic material (conjugated polymer), unlike the classical solar cells that utilize inorganic materials such as silicon. These organic materials (organic semiconductors) are characterized by having a band gap of certain gap energy (E_g), which signifies the energetic separation between the valence electrons and the nearest free electronic states, and is defined as the difference between the highest occupied molecular orbital (HOMO) and the lowest unoccupied molecular orbital (LUMO). The process of excitation and relaxation due to absorption of high energy photon is depicted in Figure 1.3.

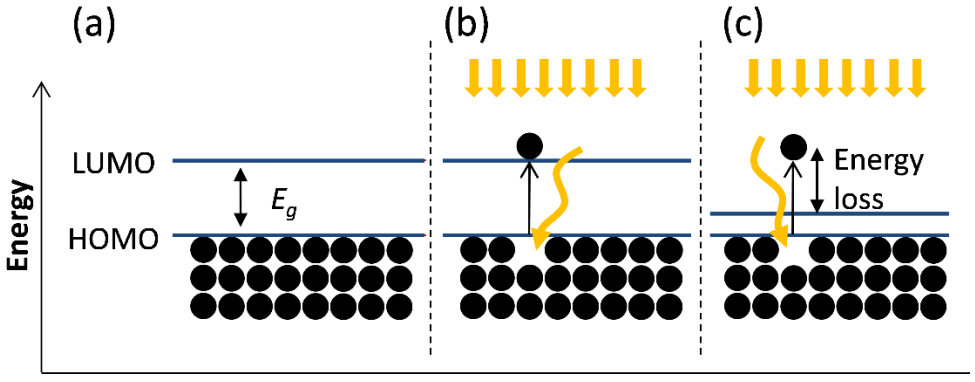

Figure 1.3 Schematic representation of the excitation process in Organic Solar cells; a) in dark b) excitation c) relaxation [17].

The interest in organic photovoltaics which has risen over the years, has general been fuelled by its offer of affordable access to electricity through flexible and inexpensive device manufacturing processes. One of its biggest attraction is the ability to be processed from solution and the applicability of fast mass printing techniques such as the roll to roll printing (typically applied in newspaper production) that allow for a high production output with a relatively low material consumption [18]. Other advantages that have been identified by researchers are; Low weight and flexibility of the PV modules, semitransparency, easy integration into other products; new market opportunities, e.g. wearable PV, significantly lower manufacturing costs compared to conventional inorganic technologies, manufacturing of OPV in a continuous process using state of the art printing tools, short energy payback times and low environmental impact during manufacturing and operations [19]. The emergence of organic solar cells was due to the discovery of conductive polymers by the working group of Alan J. Heeger, for which he was later awarded a Nobel Prize in chemistry. In his Nobel lecture, Heeger explained the importance of this discovery by saying "that they offer a unique combination of properties not available from any other known materials" indicating its promise for utility in a wide variety of applications [20]. Organic photovoltaic (OPV) cells are based on thin film polymers or small molecules (or both in some cases) and fabricated through simple, cost and energy efficient techniques, such as: spin coating, spray deposition, slot die coating, doctor blading and printing. Furthermore, cheap flexible substrates such as PET foils or even paper help to achieve cost reductions way below 1 USD per Watt peak [21]. OPVs are classified into two groups; small molecule solar cells and polymer solar cells. One of the challenges so far is reaching high modular efficiencies for their economical commercialization. According to Solarmer Energy Inc., a 10% power conversion efficiency (PCE) is required for the commercialization of OPVs and they can only achieve limits of approximately 30% PCE as defined by the works of Shockely and Queisser [19, 22, 23]. In general, progress is being made in achieving record efficiencies as new materials are synthesized and new ways of optimizing different material combinations are being discovered. Several sources give different values for record efficiencies currently held in OPVs, however in this work a chart

(Figure 1.4) published by the National Center for Photovoltaics (NCPV), a division of the American National Renewable Energy Laboratory is presented to indicate the timeline of best efficiencies achieved so far. The chart covers efficiencies achieved so far in all photovoltaic technologies from 1975 till 2015, with research facilities that have achieved such efficiencies [24]. According to this report the record efficiency is currently held by Hong Kong UST with a device efficiency of 11.5%. Though some sources have reported efficiencies as high as 13.1% these results are yet to be replicated and validated [14]. Despite these record efficiencies, OPVs are yet to attain very long device stabilities. This challenge is yet to be overcome, lifetime records of 18000 hours [25] have been reported but this is nowhere close to lifetimes obtained for their Inorganic counterparts.

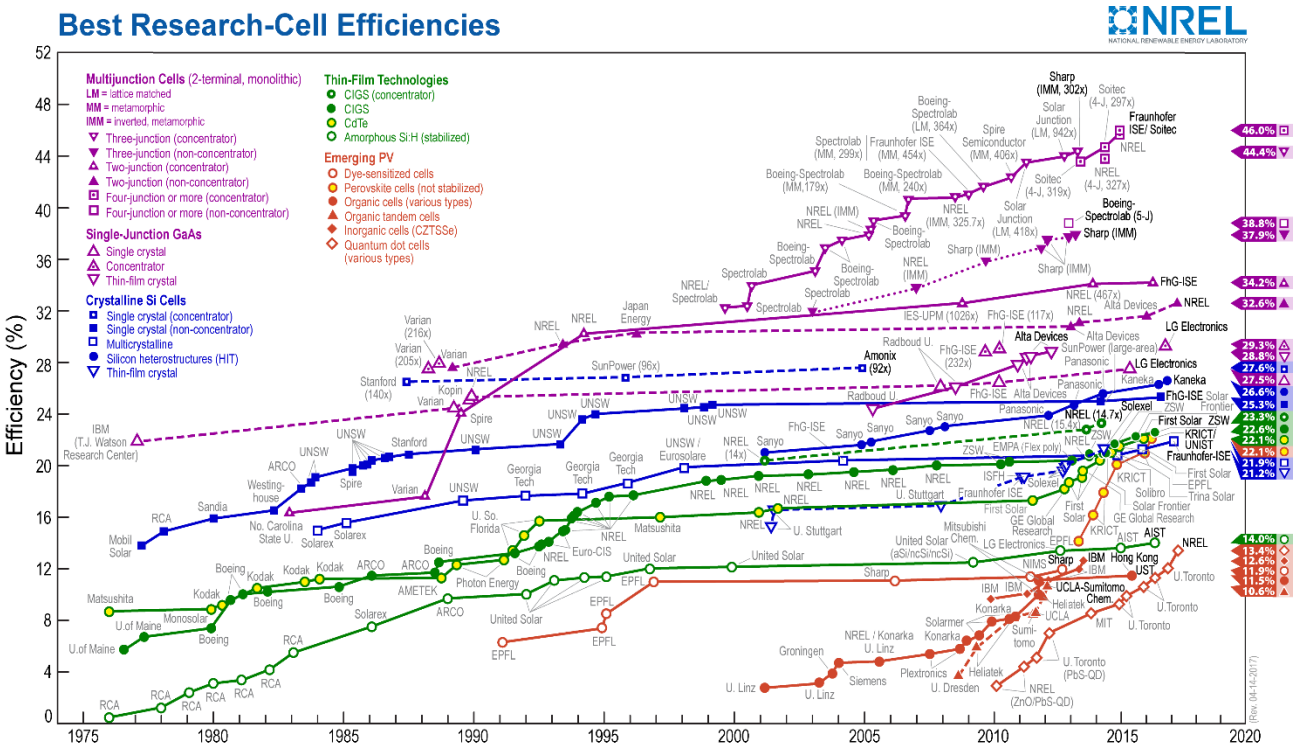

Figure 1.4 Solar cells efficiency chart from 1975 till 2015 [24].

In order to compete with their inorganic counterparts, OPVs need to gain in efficiency and attained prolonged lifetimes, this would help in achieving the various expectations placed on these devices and also enable them break into more markets already occupied by first and second generation devices.

1.3 Efficiency Determining Parameters of Solar Cells

The power conversion efficiency (η) of a solar cell is one of its most influential characteristics when discussing its performance. It is based on the parameters open circuit voltage(V_{oc}), short circuit current density (j_{sc}) and fill factor(FF). Another important parameter used to define the efficiency is the maximum power point(MPP), it is the maximum of the current-voltage product. This efficiency of an organic solar cell can be obtained mathematically as the ratio of the power generated by the device at MPP and the power of the incident radiation $P_{incident}$ as shown in Equation 1.3.

$$\eta = \frac{J_{sc} V_{oc} FF}{P_{incident}} \tag{1.3}$$

In order to ensure a globally comparable PCE for different solar cells, standardized testing conditions (STC) have been set for solar cells. The illumination value was set to 100 mW/cm^2 under an AM1.5G sun spectrum and an active layer temperature of 25 ^{o}C. As highlighted earlier, the maximum attainable efficiency is given by the detailed balance limit for inorganic p–n junction solar cells, published by Shockley and Queisser [22]. The famous Shockley diode equation (Equation 1.4) though derived for inorganic devices, has been applied by many researchers in the field of organic semiconductors to describe or fit the current–voltage characteristics. The equation is based on an exponential term, as a positive voltage bias leads to the injection of charge carriers into the solar cell. The current increases exponentially, leading to a rectifying behaviour in the ideal case. For real solar cells, however, the ideal Shockley equation was modified by two resistors. The series resistance R_s—in series with the ideal diode—basically describes and accounts for contact resistances such as injection barriers, resistance in the active layer, electrodes and also the interfacial resistance between the contacts of the active layer and the electrodes. While the shunt resistance R_{sh} accounts for leakage currents, which could arise from leakage current in the p–n junction, from the edge of the cell and by those caused by impurities in the cell. The modified version which describes the real solar cell is a function of R_s and R_{sh} and is given by equation (1.5).

$$J = J_0\left[exp\left(\frac{qV}{kT}\right) - 1\right] \quad (1.4)$$

Where, k is the Boltzmann constant, T is the absolute temperature and J_0 is the reverse saturation current density (typically in p–n junction solar cells, it denotes the current density contributed by minority charge carriers, which is the total of the hole current in the n region and the electron current in the p region) and V is the output voltage [26].

$$J = \frac{R_s}{R_s + R_{sh}}\left\{J_0\left[exp\left(\frac{q\,(V - JR_s)}{nkT}\right) - 1\right] + \frac{V}{R_{sh}}\right\} - J_{ph} \quad (1.5)$$

Where, J_{ph} is the photocurrent density, n is the diode ideality factor. When, $n = 1$, it shows that the recombination of charge carriers in the depletion region is zero (or negligible) and diffusion current is dominant in the device. However when n=2, then the reverse is the case. The characteristics of an ideal I-V curve is depicted in Figure 1.5 indicating all important photovoltaic parameters.

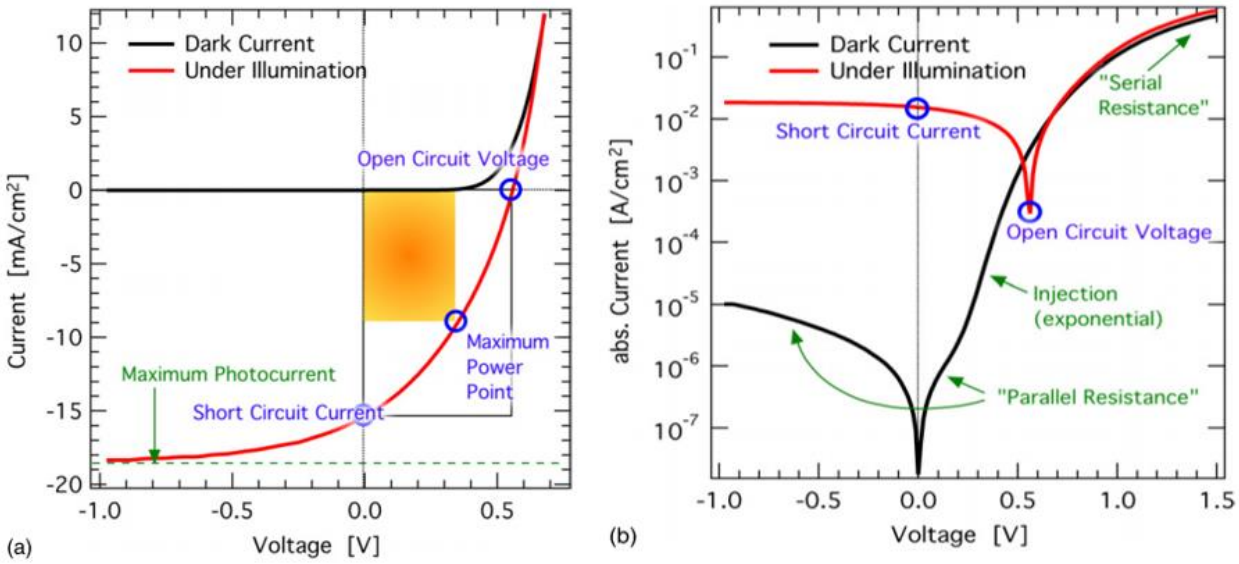

Figure 1.5 Schematic current–voltage characteristics of bulk heterojunction solar cells in (a) linear and (b) semilogarithmic representation*[27].*

1.4 Research Motivation

The focus of the master research is on application of novel electron acceptor materials in combination with well-defined conjugated polymers for yielding efficient and cost effective organic photovoltaic solar cells (OPV). The cost reduction due to use of novel and potentially very cheap acceptor materials. A given set of novel acceptor materials were classified according to their suitability for combination with the AnE-PVstat copolymer via photoluminescence characterization and application in photovoltaic devices. Optimization is to be done via proper choice of solvents and solvent additives in order to yield proper phase separation between donor and acceptor in the organic bulk heterojunction.

Combination of novel electron donors with conjugated polymers can be experimented straight-forward. However, the energetic situation at the heterojunction interface may be complicated and even based on cyclovoltammetric characterization no warrantee can be given for the compatibility of chosen donor and acceptor materials. As lately more reports were facing the scientific community that after years of absence more and more electronically non-fullerene acceptors are found and that energy losses at such interfaces tend to be smaller – when properly adapted to the donor – as compared to fullerene derivatives, the compatibility risk is balanced by a potential for high gain in performance.

1.4.1 Research Questions

- Are the given novel electron acceptors electronically and morphologically compatible for use in combination with AnE-PV stat?
- Will the use of a solvent additive influence the morphological compatibility of the donor and acceptor materials?

1.4.2 Working Hypothesis

- For proper organic solar cells, a type II heterojunction is required, in order to allow efficient charge transfer.
- Cyclovoltammetric characterization of the electron donor and acceptor materials provides first insight into whether type II heterojunctions can be formed.

- Application of the above and final proof via solar cell preparation and characterization to prove or disprove the above stated hypothesis.

1.4.3 Research relevance and justification

Present day solution-processed OPVs are based on a bulk heterojunction (BHJ) active layer, which is a blend of bicontinuous and interpenetrating electron donor (D) and electron acceptor (A) components in a bulk volume [28]. Organic solar cells have undergone a considerable rise in power conversion efficiency from 1% to >10% in the last decades [13]. Though most of the highly-efficient organic BHJ solar cells are based on chemically modified fullerenes [13], fullerenes are still limited by their weak absorption in the visible spectral region, limited spectral band width, and band gap variability, which are difficult to tune in fullerene systems by chemical modification. Also the processes involved in the production of these fullerenes are quite energy intensive. This has necessitated the quest for acceptor materials (non-fullerene acceptors) that will maintain the suitable acceptor energy levels and charge transporting qualities of fullerene derivatives while overcoming their weakness. This study aims at evaluating the possibility of increasing the absorption spectrum of OPVs by replacing the fullerene acceptors with non-fullerene acceptors and hence increasing the photo conversion efficiency of the cell. In a practical sense, it is a step towards availing affordable photovoltaics with a wide range of applications based on their flexibility to the world.

2 LITERATURE REVIEW

Organic solar cells are usually fabricated in two distinct forms depending on the positioning of the electron transport layer (ETL) and hole transport layer (HTL). This in turn affects how the charge carriers are collected and the ultimately the performance of the device. Though the importance of device architecture cannot be overstated, more important is the compatibility of the materials from which the active layer is cast and how the structure of the active layer is formed. This defines the type of heterojunction formed and the interaction of the charge carriers, how fast they can move within the bulk material without recombination. In essence casting of the active layer is the critical part of the solar cell fabrication process.

All layers of emerging solar cells should be processed from solution and fabricated using vacuum-free and low-cost processes. Solution-processed solar cells have attracted tremendous amount of attention not only because of their increasing efficiency and low cost, but also due to potential for scalability, favorable performance-to-weight ratio, easy manufacturing with low environmental impact, as well as short energy payback times [29]. This chapter therefore reviews the different architectures developed for organic solar cells, the process of formation of the junction, the influence of solvent additives and sets the precedent for the experimental part of the work.

2.1 Conduction in Polymers

Prior to the discovery of conductive polymers, polymer materials were classified as insulators based on their electrical properties. While metals were regarded as conductors and materials such as silicon were classified as semiconductors. This was largely due to the band gap of the materials were conductors had an overlapping valence and conduction band or in the case of semiconductors with a low band gap which could be overcome by some form of excitation but for the largely classified insulators the energy band gap was too large for the excitation of mobile charge carriers from the valence to the conduction band. Thanks to the discovery of conductive conjugated polymers by Alan J. Heeger, Alan G. MacDiarmid, and Hideki Shirakawa on doped polyacetylene in 1977 [30]. These

materials only become highly electrically conductive after undergoing a doping process which causes some form of structural modification process. New doors of research have opened due to this discovery, for the application of this class of materials and 40 years later more research grounds are being broken in various fields such as photovoltaics, optoelectronics.

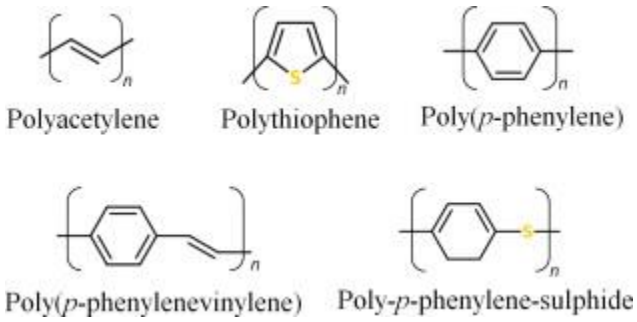

Figure 2.1 Schematic of commonly investigated conductive polymers[31]

The conduction process in polymers occurs due to the ease with which electrons move from within and between the polymer chains. This conductivity arises from the polymer's possession of a conjugated backbone, that is to say it is formed by a series of alternating single and double bonds (Figure 2.2). These alternating single and double bonds both contain a chemically strong, localized σ-bond, while the double bonds also contain a less strongly localized π-bond. The p-orbitals in the series of π-bonds overlap each other, allowing the delocalization of electrons and free movement between the atoms.

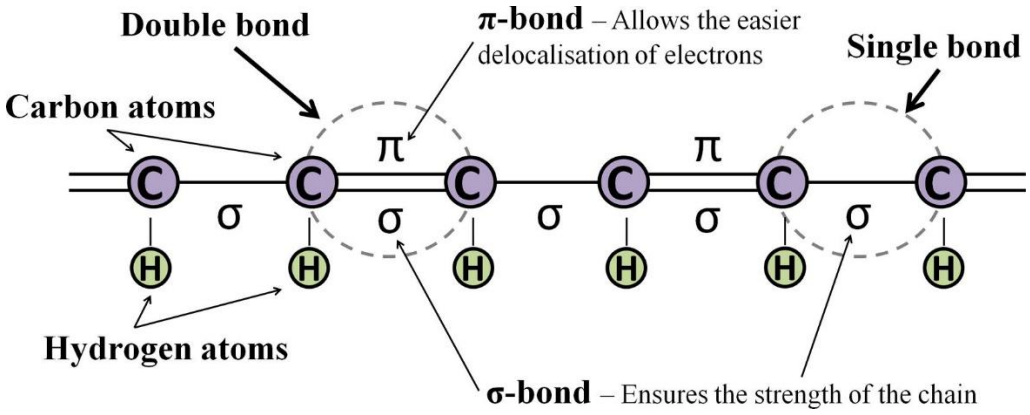

Figure 2.2 Schematic of a conjugated polymer backbone *[31].*

The delocalized electrons may move around the whole system and become the charge carriers to make them conductive [32]. Then the polymer can be transformed into a conducting form by the addition and removal of electrons from the backbone resulting in the formation of positively or negatively charged ions which then hop from one site to another under the influence of an electric field hence increasing the conductivity of the materials [32, 33]. As earlier discussed the mode of conduction is due to the delocalization of the π bonds, the π-electron system is formed by the p_z - orbitals of the sp_2- hybridized carbon atoms. Out of the four valence electrons possessed by carbon, three of them occupy the strong sigma bonds with two carbons and one hydrogen atom; and the fourth valence electron occupies the non-hybridized p_z - orbital. The overlapping π-electron wave functions together form a π-band and the degree of delocalization of these π-electrons determine the optical and electrical properties of conjugated systems. Much similar to the band gaps of inorganic semiconductors, the band gap of organic semiconductors is defined by the difference between their Highest Occupied Molecular Orbital (HOMO) and their Lowest Unoccupied Molecular Orbital (LUMO) which is analogues to the valence band and conduction band of inorganic semiconductors. This difference however depends on the length of conjugation of the polymer (number of monomer units on which the delocalized π electrons can move and contribute to charge transport) and due to the random distribution of the conjugation length, the HOMO and LUMO levels are energetically distributed which is denoted as an energetic disorder. The charge transport properties of conjugated polymer system depend on the packing of chains, the crystallinity of the solid film, concentration of impurities and structural defects, hence charge carrier mobility values of a polymer is a function of the quality of the sample [34].

2.2 Architectural Structure of Organic Solar cells

The typical structure of polymer solar cells comprises a number of layers, which gives plenty of choice for different materials and material combinations. The first layer is usually the substrate (glass, PET, paper) of the cell and accordingly the next electrode after the substrate is the front electrode. One of the requirements while building a solar cell is to

keep one of the faces transparent for illumination. It can be front face or back face illumination depending on whether the substrate is transparent or not as shown in Figure 2.3. In building a solar cell the choice of the position of the cathode and the anode is what differentiates the two available geometries – conventional and inverted – of organic solar cells. The definition of the two geometries lies within the direction of the charge flow [12].

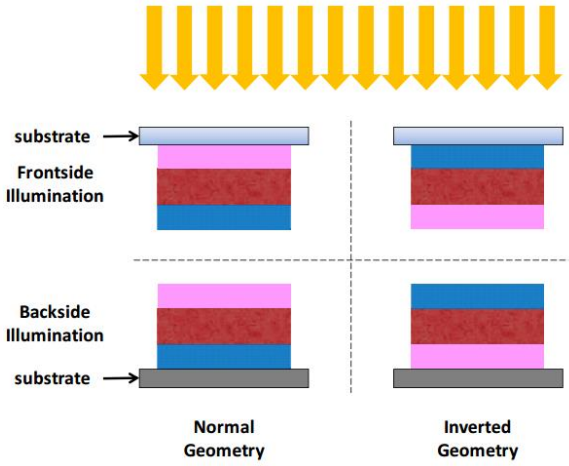

Figure 2.3 Different geometries of OPV devices with frontside or backside illumination [12].

2.2.1 Conventional Geometry

In a conventional solar cell, the substrate and the transparent electrode on it is the positive electrode, with the light passing through the substrate and this electrode before being absorbed in the active layer. The top electrode is then the negative electrode. The normal device in the laboratory scale as seen in Figure 2.4, usually, consists of the following components: a glass substrate, a bottom indium tin oxide (ITO) thin film coated on the glass substrate, forming the anode, which is transparent to solar radiation, a buffer layer usually poly (ethylenedioxythiophene) blended with poly (styrenesulphonate) (PEDOT:PSS) with hole-conducting property, a photoactive layer (a mixture of conjugated polymers and acceptor materials), a second buffer layer with electron-transporting capability, and a top metal cathode, with a low work function to drain and collect electrons [29, 35]. The cathode in normal geometry is deposited by thermal evaporation or sputtering, and is susceptible to degradation by oxygen and water vapor [36]. Also, the

PEDOT: PSS layer is hygroscopic and acidic [37], the hygroscopic nature causes an ingress making it detrimental to the polymer active layer, while its acidity affects the ITO layer.

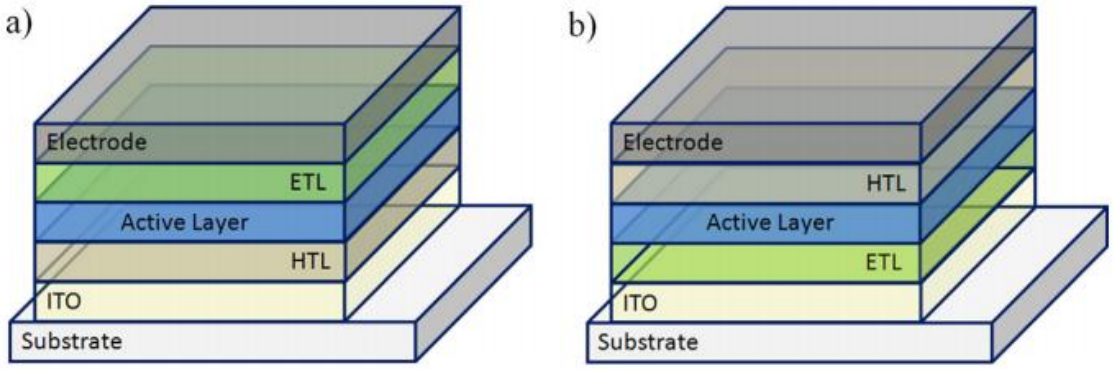

Figure 2.4 Different device architectures of bulk heterojunction solar cells. (a) Standard (conventional) device design and (b) inverted device architecture *[19]*

2.2.2 Inverted Geometry

In the inverted geometry, the two electrodes and the charge selective layers are switched around, such that the transparent electrode at the substrate is the negative electrode, with an electron transport layer (ETL) between it and the active layer, while the top electrode is the positive electrode with a hole transport layer (HTL) between it and the active layer (Figure 2.4). The polarity of charge collection, is the opposite to that of the conventional or normal architecture, allowing the use of higher work function (Ag, Au) and less air-sensitive metals as the top electrode for hole collection.

2.3 Layer Junctions in Organic Solar Cells

In organic semiconductors, the binding energy of the excitons ranges from 0.1-1eV which is relatively large when compared to Silicon (In silicon the electron is split by the thermal energy of the lattice which is approximately 25 meV at room temperature and the binding energy of electrons in most inorganic semiconductor is well below 25 meV) and as such the built in electric fields are not high enough to dissociate the excitons directly. This necessitates the introduction of a process that efficiently dissociates the bound electron-hole pairs. This is possible at the sharp drop of potential at donor–acceptor (D-A) as well

as semiconductor–metal interfaces [38]. Overtime different interfaces have been developed to enhance exciton dissociation efficiency and increase charge transport efficiency which in turn translates to more efficient devices. There are fundamentally four types of junctions that have been reported for organic solar cells; (1) Single Layer; (2) Bilayer; (3) Bulk Heterojunction; (4) Diffuse Bilayer. Remarkable improvements in device efficiency have been achieved due to progress in tuning and achieving finely mixed bulk heterojunction photoactive layers. This makes the BHJ the most commonly investigated device interface in recent years. The different designs of Junction interfaces are discussed in the following subsections.

2.3.1 Single Layer Junction

The first organic solar cells were based on single thermally evaporated molecular organic layers sandwiched between two metal electrodes of different work functions typically Indium Tin Oxide with a higher work function and a metal of lower work function such as Aluminum or Magnesium as seen in Figure 2.5. They are the simplest form of organic photovoltaics. The rectifying behavior of these devices can be explained by the MIM-model (for insulators) or by the formation of a Schottky barrier (for doped materials) between the metal with the lower work function and the p-type organic layer [38].

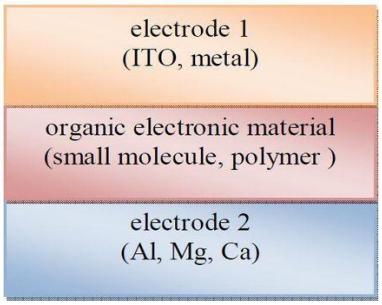

Figure 2.5 Schematic of a Single Layer Organic Cell [39]

An electric field is set up in the active layer by the difference in the work function of the two metals. When light is absorbed by the active layer and excitons are formed, the potential created by the different work functions helps to split the exciton pairs, pulling electrons to the positive electrode and holes to the negative electrode [40, 41]. Since the

exciton diffusion length for most organic solar cell materials is below 20 nm, only those excitons generated in a small region within ≤20 nm from the contacts contribute to the photocurrent. Due to the high series resistances, these materials show a low FF and a field-dependent charge carrier collection. It is reported that such thin film devices can work well as photodetectors, as under a high reverse bias the electric field drives the created charges to the electrodes [38]. Different researchers have designed devices based on this layer structure and obtained poor results for the photovoltaic parameters, conjugated polymers were used in this type of photovoltaic cell. One device used polyacetylene as the organic layer, with Al and graphite, producing an open circuit voltage of 0.3 V and a charge collection efficiency of 0.3% [42]. An Al/poly(3-nethyl-thiophene)/Pt cell had an external quantum yield of 0.17%, an open circuit voltage of 0.4 V and a fill factor of 0.3 [43]. An ITO/PPV/Al cell showed an open circuit voltage of 1 V and a power conversion efficiency of 0.1% under white-light illumination[44]. A major limitation of this type of active layer junction is that the electric field resulting from the difference between the two conductive electrodes is seldom sufficient to split the excitons. Often the electrons recombine with the holes without reaching the electrode.

2.3.2 Bilayer Heterojunctions

In a bilayer device, a donor and an acceptor material are stacked together and the charge separation occurs at the planar interface created by this stacking. The charge separation is facilitated by a large potential drop between donor and acceptor. As in the case of the single layer, the bilayer is sandwiched between two electrodes matching the donor HOMO and the acceptor LUMO, for efficient extraction of the corresponding charge carriers (Figure 2.6). The two layers used usually have different electron affinity and ionization energies, therefore electrostatic forces are generated at the interface between the two layers. The materials are chosen to make the differences large enough that these local electric fields are strong, which splits excitons much more efficiently than single layer photovoltaic cells. The electron acceptor layer has a higher electron affinity and ionization potential, and the other layer is the electron donor. This structure is also called a planar donor-acceptor

heterojunction [40, 41, 45, 46]. One major advantage it possesses over the single layer device is the monomolecular charge transport. After the excitons are dissociated at the materials interface, the electrons travel within the n-type acceptor, and the holes travel within the p-type donor material. Hence, holes and electrons are effectively separated from each other, and thus charge recombination is greatly reduced and depends more on trap densities.

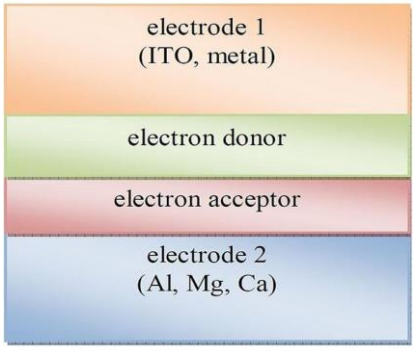

Figure 2.6 Schematic representation of the Bilayer Solar cell configuration [39]

Bilayer devices can be produced either by sequential thermal deposition of pigments, by solution casting of one soluble material and evaporation of a second layer, or by sequential solution casting applying a polymer precursor route[38]. A typical example of a good acceptor material that could be used for such devices is C_{60} because of its high electron affinity. A C_{60}/MEH-PPV Bilayer cell was investigated and had a relatively high fill factor of 0.48 and a power conversion efficiency of 0.04% under monochromatic illumination[47]. In 1986 Tang reported Organic solar cells fabricated from copper phthalocyanine and a perylene tetracarboxylic derivative (two conjugated small molecules), and achieved a power conversion efficiency of about 1% more interesting about this device is the relatively high fill factor obtained around 0.65 and the fact that the charge generation efficiency was independent of the bias voltage[48]. Furthermore, power conversion efficiencies of about 3.6% under Sun AM 1.5 solar illumination with this structure were reported with an evaporated bilayer device using copper phthalocyanine and C_{60} [49, 50]. This device structure though more advantageous than the single layer structure

has a major limitation of also limited excitons reaching the interface, this because a typical active layer needs to be 100nm thick to allow effective absorption of photons but the exciton diffusion length is only to the order of 10-20nm.

2.3.3 Diffuse Bilayer Heterojunction

The Diffuse bilayer heterojunction has a structure that is in-between the bilayer and the bulk heterojunction. Its structure is aiming to adapt the advantages of both concepts, an enlarged donor–acceptor interface and a spatially uninterrupted pathway for the opposite charge carriers to their corresponding electrodes. A diffuse interface is achieved in different ways: (i) Solution processed; two thin polymer films can be pressed together in a lamination procedure applying moderate pressure and elevated temperatures [51]. (ii) It can also be achieved by spin coating the second layer from a solvent that partially dissolves the underlying polymer layer [38, 52]. (iii) Lastly, through a controlled interdiffusion between an acceptor fullerene and a donor polymer by annealing of a bilayer device an intermixed interfacial region could be achieved [38]. Earlier researchers [51] reported calculated power conversion efficiencies approaching 2% were reported for the laminated polymer: polymer device for simulated AM 1.5 conditions. However with advancements in processing methods better efficiencies are being reported, Loiudice et al [53] reported 4.0% PCE in a diffuse bilayer device as against 2.7% obtained from a BHJ of same similar material system. This improvement in efficiency was achieved by a sequential coating of the donor (i.e., P3HT) and acceptor (i.e., [6,6]-phenyl-C_{61}-butyric acid methyl ester, PCBM) species from orthogonal solvents. The doping of P3HT with the electron acceptor, F_4-TCNQ, was carried out through a solution coblending process prior to its casting.

2.3.4 Bulk Heterojunctions

The active layer (also commonly called absorber layer) of an efficient state of the art bulk heterojunction solar cell is made of so-called donor and acceptor molecules [19]. The concept of the bulk heterojunction (BHJ) was introduced to address the limited exciton (tightly bound electron hole pair) diffusion length in organic solar cells, which had been a problem for previous organic solar cells. It is an interpenetrating group of donor and

acceptor materials introduced to reduce the average distance between donor and acceptor molecules without reducing the overall thickness of the device active layers.

In a BHJ, the donor and the acceptor are mixed to form a polymer blend with the distance scale between the donor and the acceptor similar to the exciton diffusion length. The domain sizes of this blend are on the order of nanometers, allowing for excitons with short lifetimes to reach an interface and dissociate due to the large donor-acceptor interfacial area. The excitons generated in either material may reach the D–A interface more readily for efficient disassociations. The electrons then move to the acceptor domains and are carried through the device to be collected by one electrode, while the holes are pulled toward the opposite direction to be collected at the other side. BHJs are similar to bilayer heterojunctions but have higher quantum efficiencies compared to the bilayer heterojunction, because in BHJ it is more likely for an exciton to find a D–A interface within its diffusion length as a result of the simplicity in achieving thick enough layers for absorption without the challenge of obtaining a layer structure with similar levels of performance.

Recently, there have been several advances to the processing methods of the active layer in an attempt to control its morphology. This attempt however has been limited by the random nature in the phase separation process due to the three-dimensional morphological structure in the D-A blends posing a fundamental challenge for the bulk HJ structure [18]. Considering that the high interfacial facilitates the exciton diffusion process, even for active layers thicker than the exciton diffusion lengths an important step to achieve higher efficiencies in the BHJ structure will be to control the morphological structure to achieve the optimal spatially distributed exciton dissociation interfaces and charge transport channels [18].

Several unfavorable structures such as too large aggregation in the bulk HJs may be formed during phase separation, which can lead to less interface for exciton separation or charge trapping when there are many isolated domains with no contact to the respective electrode. These large domains by the above processes limit charge generation but on the positive

side help to reduce bimolecular recombination. The degree of phase segregation depends strongly on the intermolecular interactions and the processing conditions. There is still no agreement on how an ideal nano-morphology of a bulk heterojunction should look like. A very fine dispersion of the acceptor in the donor material will lead to efficient charge generation but poor charge transport. Ideal charge transport could be achieved by arranging the donor and acceptor in by bilayer stack (Figure 2.6). On the other hand, charge generation happens only at the interface between the two layers and will be overall poor. Calculations and morphology simulation work have suggested that the arrangement shown in Figure 2.7b should lead to ideal performance [19]. Highly ordered donor and acceptor domains will ensure excellent charge transport and a combination with a domains width equal 2 times the exciton diffusion length can equally foster efficient charge generation at the same time. The ideal structure is not easily achieved, however, connected phases are formed with either donor or acceptor material dissolving in the others' domain. A cross-section of "real" bulk-heterojunction solar cell is sketched in Figure 2.7 (a)

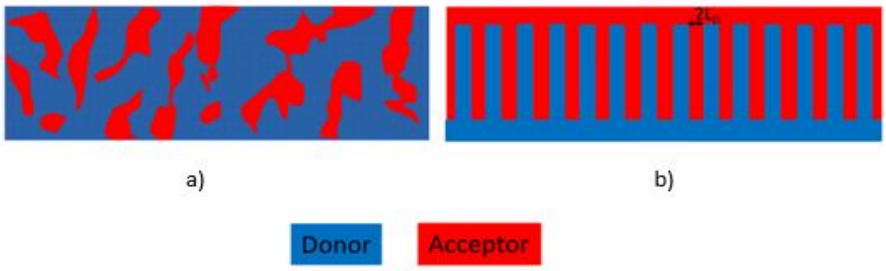

Figure 2.7 Schematic representation of the Real BHJ (a) and Ideal BHJ structure (b) *[19]*.

The concept of BHJs is implemented by solution processing of a polymer–acceptor (either fullerene or more recently developed non-fullerene acceptor materials) blend or by co-evaporation of conjugated small molecules. Bulk heterojunctions have the advantage of being able to dissociate excitons very efficiently over the whole extent of the solar cell, and thus generating electron–hole pairs throughout the film [27].

The first solution processed BHJ structure was independently reported in 1995 by the groups of Heeger and Friend [54], the structure was achieved using polymer–fullerene and

polymer–polymer blends, respectively, which has now become the predominant structure for solution-processed OPV devices. Since these first reports different research groups have employed different processing conditions and applied post deposition treatments to influence the phase separation. In solution processed organic solar cells, the D-A network structure of the BHJ formed is greatly influenced by the properties of the solvent such as vapour pressure, boiling point and molecular polarity.

Furthermore, the use of solvent additives and anti-solvents have proven useful in increasing the degree of charge separation, level of ordering and charge transport [55]. Thermal and solvent annealing are also examples of post deposition treatments [56] that could be applied to the active layer to improve the morphology by the increased crystallinity of either the donor or acceptor phases which in turn leads to higher power conversion efficiencies through increased charge transport to the electrodes. The role morphology plays in improving device performance has been emphasized by several authors [18, 27, 38], while the manifold increase has been reported in power conversion efficiencies through the application of novel processing steps the optimization of the morphology is still an ongoing process. Previous studies on coevaporated copper phthalocyanine/fullerene solar cells indicated an increase in efficiency up to 5.0% by utilizing a planar-mixed heterojunction [57], and also by the application of different novel materials and optimization by solvent additive, solution-processed polythiophene: fullerene cells have achieved between 6% and 8% efficiency [58-60].

2.4 Working Mechanism of Bulk Heterojunction Organic Solar Cells

The working mechanism of BHJs can be described in four distinct steps [27, 38, 46]: (1) light absorption and generation of highly localized, tightly bound Frenkel excitons; (2) exciton diffusion to the donor−acceptor interface; (3) exciton dissociation at the interface, first creating charge transfer (CT) states or so-called polaron pairs; then CT states fully dissociate into free charge carriers; (4) charge transport and collection. These steps are depicted in Figure 2.8 below and are described in detail in the following subsections;

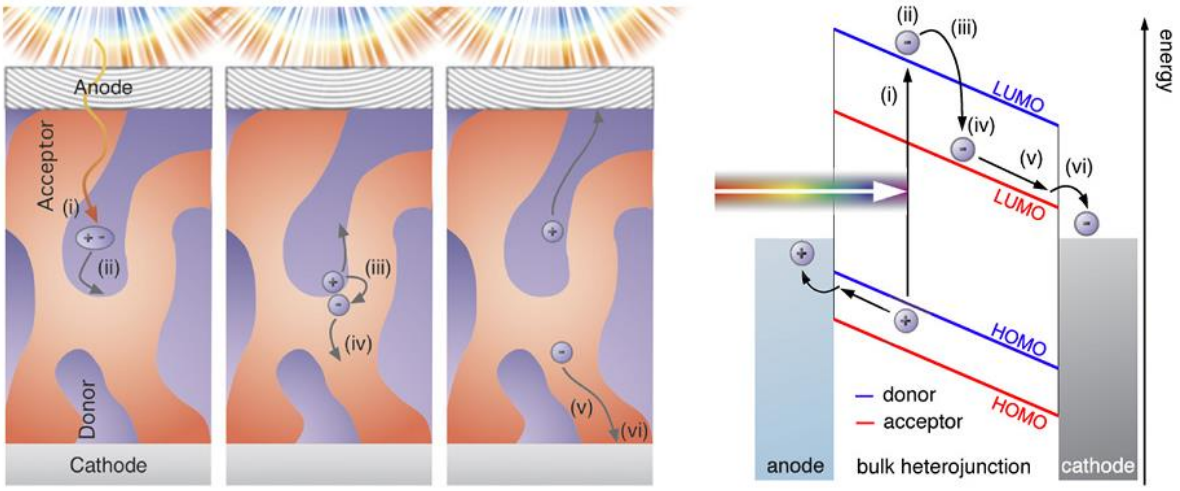

Figure 2.8 Schematic of the process of current generation in an organic solar cell. Left: kinetic depiction, right: energy diagram. (i) singlet exciton generation from an absorbed photon in the donor material. (ii) exciton diffusion to the acceptor interface. (iii) Exciton dissociation by electron transfer to the electronegative acceptor molecules. (iv) separation of the still Coulomb-bound electron–hole pair due to electric field and material disorder. (v) Charge transport of electron (vi) extraction of the charges: photocurrent *[27]*.

2.4.1 Light Absorption and Exciton Generation

Light is usually absorbed in the donor material of donor-acceptor type Organic Solar Cells (OSC), hence the absorption efficiency of an OSC is, to a great extent, determined by how closely the spectral response of the polymer matches with the solar spectrum [27, 46]. Organic semiconductors exhibit absorption coefficients higher than 10^7 m^{-1} making absorption possible in very thin layers of about 100-300nm. This is unlike the inorganic semiconductors which require more layer thickness for good absorption. However, many organic materials have a rather narrow absorption width. Conjugated polymers commonly used in organic solar cells typically cover the visible optical spectrum only [61-63], while the inorganic semiconductors (silicon and $CuInSe_2$) absorb across the whole visible spectrum of the sun light, and beyond to more than 1000 nm (optical bandgap 1.1 eV). Low light absorption efficiency leads to low photocurrent production, this is a limitation for currently high performing solar cells as their absorption does not match with the solar spectrum. An example is P3HT which has a band gap of 1.9 eV, and is only able to harvest

up to 22.4% of the available photons[46], this has resulted in increased research in materials with better aligned energy levels for better light harvesting capabilities. Hence, low band gap OSC materials are needed to optimize photon collection [46]. A low band gap polymer can be defined as a polymer with a band gap below 2 eV, which absorbs light with wavelengths longer than 620 nm. These polymers materials have the possibility to improve the efficiency of OSCs due to a better overlap with the solar spectrum and this increases photocurrent considerably [46].

Upon absorption of photons by the active layer, coulomb-bound electron-hole pairs (known as excitons) are generated. In organic materials, excitons usually reside on one molecule or along an extended polymer chain segment, intrachain excitons [64], although in some cases, interchain excitons residing on adjacent molecules are reported [65]. The combined spin state of the two charges forming an exciton has high importance. Singlet excitons have a resulting spin of zero, and triplet excitons have a spin of 1—which is possible in three different combinations, thus the name. Singlet excitons can be generated upon illumination, which is due to specific selection rules. In contrast, both singlet as well as triplet excitons can be formed due to interaction following charge injection [27]. Excitons are characterized by certain lifetimes, upon exhaustion of which they recombine radiatively. For singlet excitons in organic semiconductors, the lifetime is around 1 ns, with photoluminescence as the subsequent decay path [27]. The excitons generated in organic solar cells are the primary excitation following the absorption of photons, exhibiting a significant binding energy much larger than the thermal energy which is why they are known as Frenkel excitons (weakly bound type is called Wannier–Mott). For weakly bound excitons, the thermal energy at room temperature would be sufficient for dissociation. Since the excitons formed have binding energy much larger than the thermal energy in organic semiconductors, another driving force is needed to dissociate them [27]. This additional driving force can easily be achieved at the interface between two different molecules exhibiting an energy level offset in the range of or larger than the exciton binding energy of the constituting organic semiconductors. The semiconductor material exhibiting higher

molecular energy levels—specifically the lowest unoccupied molecular orbital (LUMO) but also the highest occupied molecular orbital (HOMO)—is then called the (electron) donor, whereas the other is called the (electron) acceptor, the combination of these gives a typical **TYPE II heterojunction (**Figure 2.9**)** [66]**.** The formation of this type II heterojunction enables efficient electron transfer from the donor to the acceptor, which may be accompanied by the formation of charge transfer (CT) states, where the electron is located on the acceptor LUMO and the hole on the donor HOMO.

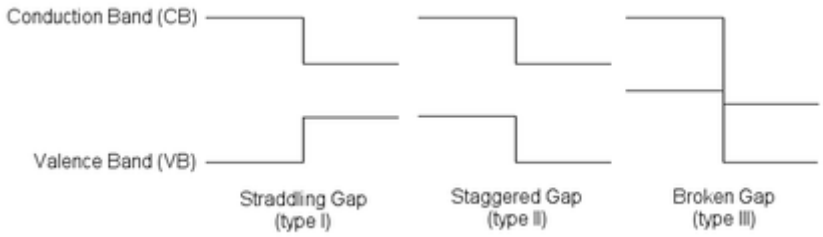

Figure 2.9: Heterojunction interfacial structures

2.4.2 Exciton Diffusion to Donor-Acceptor Interface

The diffusion length of an exciton invariably determines the possibility of the exciton's diffusion to the interface. This is usually denoted as L_D, excitons with longer L_D have better chances to reach the D–A interface. Exciton diffusion lengths in polymeric materials have been measured and reported by researchers to be between 1–10 nm [67-69]. Only the photons absorbed within this range of distances from the interface can contribute to the device photocurrent generation. The number of excitons that can reach the interface and dissociate into carriers will be maximized if the layer thickness is within the range of their diffusion lengths. However, the absorption of the polymer layer is limited by thickness and as such it requires a minimum of 10nm to absorb enough light [19, 46]. Excitons generated further away from the planar interface to the acceptor than the exciton diffusion length are lost by recombination—usually radiative in the form of photoluminescence. The short diffusion length of the excitons necessitated the development of the BHJ which was reported by Yu et al [54] which adopts the short diffusion lengths. As discussed in the previous section, the BHJs promote an intermixing of the materials and in simple terms allows the interface to be close to the generated excitons. The investigations of Yu et al

[54] led to a 10 fold increase in the incident photon to electron conversion efficiency obtained by blending the donor (poly(2-methoxy-5-(2'-ethyl-hexyloxy)-1,4-phenylene vinylene)) (MEH-PPV) and acceptor (Fullerene C_{60}) molecules in the photoactive layer as against the results from the conventional Bilayer heterojunction. The majority of research efforts have been focused on decreasing the distance between donor and acceptor instead of searching for new molecules to increase diffusion lengths [46]. Some research groups have made efforts to investigate and propose methods for increasing the diffusion length of excitons (L_D), Paul et al. [70] proposed a method for increasing the exciton diffusion length by converting singlet excitons into long-lived triplets. By doping a polymer with a phosphorescent molecule, they have demonstrated an increase in the exciton L_D of a polymer from 4 to 9 nm. Once the excited state—diffusing within the donor phase—has reached the interface to the acceptor material within its diffusion length, it can transfer its electron to the electronegative acceptor as seen in Figure 2.10a. This charge transfer is reported to be extremely fast, on the order of tens of femtoseconds [27]. After the diffusion to the interface the excitons need to be dissociated into charge carriers and this is achieved by an internal electric field. The charge generation process consists of exciton generation mostly in the polymer, energy (not electron) transfer to the acceptor and subsequent hole transfer to the polymer. The process of charge transfer, possible loss mechanisms through photoluminescence or intersystem crossing (ISC) and energy transfer is depicted schematically in Figure 2.10 below.

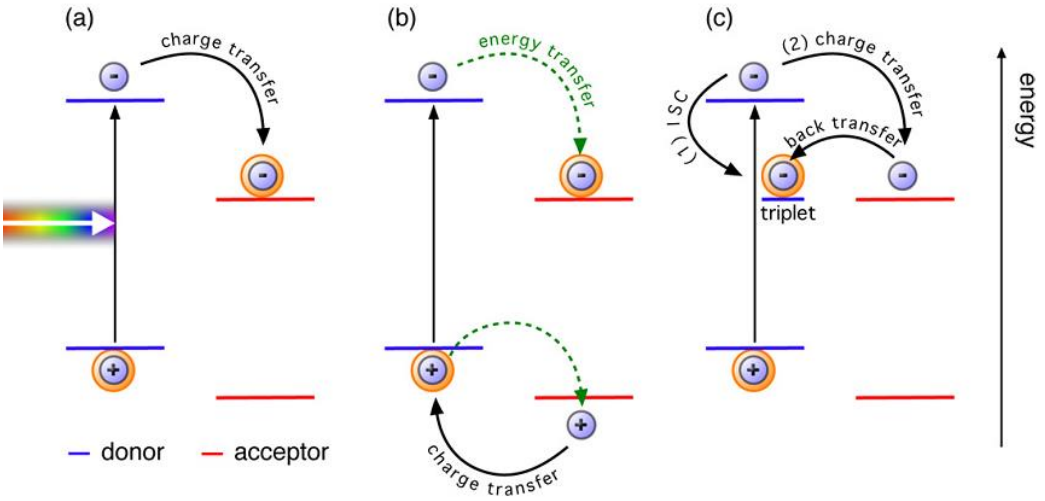

Figure 2.10 Typical charge transfer reactions in organic solar cells [27].

The reaction processes that occur in Figure 2.10 are described as follows (a) The singlet exciton on the donor material is dissociated by an electron transfer to the acceptor material. The final state is indicated by the frame of the charge carriers. (b) Forster energy transfer of the exciton from donor to acceptor, followed by a hole transfer from acceptor to donor. The final state is similar to case (a). (c) Triplet excitons can act as loss mechanisms in two ways: (1) If ISC is faster than the charge transfer, the singlet exciton is converted to a triplet, which decays subsequently. (2) If the electron–hole pair resulting from the electron transfer cannot be separated, an electron back transfer to a triplet exciton level in the donor can take place. In (1) and (2), no charge carriers are generated

2.4.3 Exciton and Charge Carrier Dissociation

The differences in Electron Affinity (EA) and Ionization Potential (IP) between donor and acceptor layers set up electrostatic forces at the interface. When chosen properly, the electric fields generated from such differences can break up the excitons into electrons and holes efficiently [46]. With a type II (staggered) heterojunction energy level alignment at the donor–acceptor interface, a photo-generated exciton near this interface may dissociate through a rapid electron transfer process [71], resulting in separated holes in the donor HOMO level and electrons in the acceptor LUMO level. To allow the electron transfer process to be energetically favorable, the LUMO (or HOMO) level offset at the interface

needs to be greater than the exciton binding energy [18]. Once the singlet exciton has been dissociated with the help of a suitable acceptor material, electron and hole reside on the acceptor and donor material respectively, but are still Coulomb bound [27]. This negative and positive polaron (an electron or a hole, in combination with a distortion of the charge's environment) coulomb bound pair also known as a polaron pair need to be separated to obtain free charge carriers [27]. The Braun–Onsager model is used to model the polaron pair separation. The model was initially developed in 1938 by Onsager - It was used to calculate the probability to separate a Coulomb-bound pair of ions of opposite charge with a given initial distance under the assistance of an external electric field, he theorized that the effect of an electric field is to increase the fraction of escaping ions by a factor which in the development stage of the effect is proportional to the field intensity and independent of the initial distance, although it depends on the orientation of an ion pair [72]. However this model was extended by Braun forty-five years later- accounting for the finite lifetime of the initial bound state, and applied it to the dissociation of charge transfer states in donor–acceptor HJs [73]. The Braun–Onsager model is shown schematically in Error! eference source not found.. There are two possible paths the polaron pair can take, it either recombines to the ground state with a constant rate, given by its inverse lifetime $k_f = \tau_{pp}^{-1}$, or it dissociates to free charges with the rate k_d. Free charges can meet to generate bound polaron pairs again with the rate k_r. The probability of dissociation as given by the Braun-Onsager model is given below in equation 2.1;

$$P(F) = \frac{K_d(F)}{K_d(F) + K_f} \tag{2.1}$$

Where, F is the electric field and $k_f = \tau_{pp}^{-1}$ the recombination rate of the polaron pair to the ground state. The field dependent dissociation rate k_d (F) is given by equation 2.2,

$$K_d(F) = \frac{3\gamma}{4\pi r_{pp}^3} exp\left(-\frac{E_b}{KT}\right)\frac{J_1\left(2\sqrt{-2b}\right)}{\sqrt{-2b}} \tag{2.2}$$

Where. $\gamma = {}^{q\mu}/_{\in\in_0}$ is the Langevin recombination factor, μ is the sum of electron and hole charge carrier mobility, r_{pp} is the initial polaron pair radius, $E_b = {}^{e^2}\Big/_{4\pi \in\in_0 r_{pp}}$ is the

Coulomb binding energy of the pair, kT the thermal energy, J_1 the Bessel function of order one, and

$b = \frac{e^3 F}{(8\pi\epsilon\epsilon_0 (KT)^2)}$ e is the elementary charge, and $\epsilon\epsilon_0$the effective dielectric constant of the organic semiconductor blend. It is interesting to note that the polaron pair dissociation probability, contains mobility and polaron pair recombination rate in linear dependence, so that the μτ product is decisive for the dissociation yield.

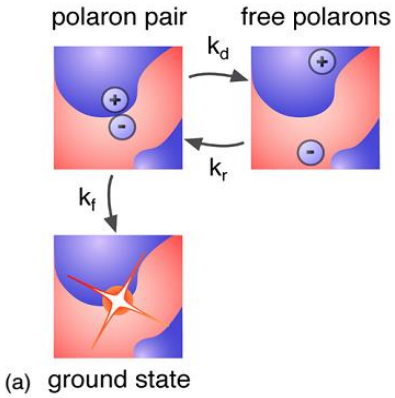

Figure 2.11: Schematic representation of the interplay between dissociation of polaron pairs to free charges with rate kd—the reverse process of free polaron recombination, connected by detailed balance, going with rate kr—or recombination of the polaron pair to the ground state with rate kf.

A major drawback of Braun–Onsager model is that the parameters r_{pp} and k_f are mostly used as fit factors in order to align with experimental data such as photocurrents, this is because the Braun–Onsager model does not account for energetic disorder or high local charge carrier mobilities due to polymer chains or nanocrystalline regions in either the donor or acceptor phase [27]. However, the recently developed Monte Carlo simulation explained the effect of extended polymer chains on the dissociation yield [74] and considered energetic disorder as well as effective conjugation lengths of ten monomer units [75]. The dissociation yields of both models were compared [27] and the increased conjugation length had an impact on the separation yields. The fraction of polaron pairs which cannot be dissociated, in some cases recombine geminately—a monomolecular process, which is proportional to the polaron pair concentration, as against the product of electron and hole densities. The loss process is either non-radiative or has a very low

emission cross section. In the case that the polaron pair cannot escape the mutual influence, e.g. due to a too intimate mixing leading to very fine-grained interfaces, one possible process is an electron back transfer from the acceptor to a triplet exciton state, as indicated in Figure 2.10c.

2.4.4 Charge Carrier Transport and Extraction

This is the final step in the conversion of solar energy to electricity in an OSC device. In this step the generated free charge carriers are transported to the electrodes where they are then collected to give electricity. In donor–acceptor solar cells, the donor material is mostly hole conducting transporting the positive charge carriers through an electrochemical gradient driven diffusion and drift due to a built in electric field, whereas the acceptor transports the electrons [27]. As a charge travels to the electrode, it can recombine or become trapped in a disordered interpenetrating organic material and thus causes efficiency drop [46]. Due to the lack of long-range order in the solution-processed and evaporated organic semiconductors, the electrical transport mostly takes place by hopping from one localized state to the next where charge carriers are localized and may only sample a finite number of locations within the overall density of states, instead of band transport found in crystalline semiconductors. Hence, it becomes paramount that the charge carriers have a high mobility to prevent bimolecular recombination [76]. Bimolecular recombination results from the buildup of free electrons and holes in the BHJ active layer. One of the most important factors is the hole mobility (μ_h) of the donor and electron mobility (μ_e) of the acceptor. It plays a major role in determining the electrical conductivity (σ_c) given by;

$$\sigma_c = ne\mu \tag{2.3}$$

The charge transport within an OSC can be described by the following equations for charge carrier velocity v and current density j:

$$v = \mu.F, \tag{2.4}$$

$$j = j_{drift} + J_{diffusion}, \tag{2.5}$$

$$j_{drift} = e.n.\mu.F, \tag{2.6}$$

$$j_{diffusion} = D\frac{\partial n}{dx} = \mu\frac{kT}{e}\frac{\partial n}{dx}, \tag{2.7}$$

Where, μ is the charge carrier mobility, n the number of carriers and F is the electric field. The total current density j in a solar cell is the sum of the drift currents driven by electric field j_{drift} and by diffusion $J_{diffusion}$ driven by the concentration gradient $\frac{\partial n}{dx}$ of the carriers. The drift distance of the charge carriers photo-generated anywhere in the active layer is given by,

$$d_m = \mu\tau\left(\frac{V_{bi}}{L}\right) \tag{2.8}$$

Where, τ is the charge carrier lifetime, V_{bi} is the built-in voltage due to the work function difference between the electrodes and L is the active layer thickness of the device [77]. When, $L > d_m$, the device will begin to have losses during charge transport, so mobility is also important in device fabrication. Because of these reasons, high mobility is a vital component of highly efficient donor polymer systems [76]. Upon successful transport of charge carriers, they are extracted and this extraction process is driven by an internal electric field across the photoactive layer caused by the different work function electrodes for holes and electrons as well as by diffusion. This difference in electrode work function is generating the internal electric field that drives the drift current under photovoltaic operation. The main electrode parameters characterizing efficient charge carrier extraction are:

1. Selectivity only to the respective charge carriers;
2. Formation of an ohmic contact with respective charge carrying materials [78, 79].

Thus the work function of an electrode must be aligned to HOMO or valence band, and LUMO, conduction band, of hole-conducting donor and electron-conducting acceptor materials, respectively. The solar cell performance therefore depends significantly on

choice of electrodes as the charge recombination at the semiconductor/electrode interface is a factor that limits device performance.

2.5 Influencing Nanomorphology of the Active Layer in Solution Processed OSCs

As stated in the previous section the morphology of the active layer is of major importance in bulk heterojunction solar cells [80]. Due to the tradeoff between exciton dissociation—where a fine grained phase segregation is ideal—and charge transport—where a bilayer configuration is optimum—the size of domains formed by the donor and acceptor material are therefore very crucial to device performance [76, 81]. The morphology of the BHJ blend in solution processed OSCs can be fine-tuned by controlling the liquid-liquid phase separation during the film formation or by subsequent treatment of the solid BHJ film. The following parameters have been identified as significant for their influence on the nanoscale morphology of the BHJ blends:

a) Solvent from which the BHJ composite is cast;

b) Ratio between the polymer and fullerene in the BHJ film;

c) Chemical additives (with differential solubility)

d) Concentration of the solution (% solids);

e) Control of phase separation by thermal and/or solvent annealing;

f) Molecular structure of the materials [38, 80, 82].

The molecular structures of the conducting polymer (or small conjugated molecules) and fullerene determine their solubility in organic solvents and their miscibility in solution. The use of different organic solvent influences the drying time during film formation based on the boiling points of the organic solvents [46, 82]. Thermal and/or solvent annealing enable the crystallization and diffusion of one or both components in the BHJ blend leading to de-mixing and coarsening of the phase separation [82]. Heterojunction with controlled growth can reach a structure called the ordered heterojunctions (OHJs). OHJs provide better control over the D–A materials positioning, which results in better QE than that of highly

disoriented heterojunctions, and therefore may be the next logical step beyond BHJs [46]. Film morphology can also have a drastic effect on the quantum efficiency (QE) of the device, by simply engineering good film morphology there is a possibility of increasing QE and as a result the performance of the device. Rough surfaces and presence of voids can increase the chance of short circuiting. They also raise the series resistance and thus reduce the current output. Though the BHJ structures is designed to reduce distances between excitons and D–A interfaces, when this is structure is amorphous and disordered it leads to charge recombination [46]. An ideal morphology consists of both laterally and vertically phase separation, which should both be optimized for satisfying device performance [46, 80]. In general the influence of casting solvents have been researched extensively by different research groups [80] and reported to be critical to the film morphology of solution processed organic solar cells, hence this work discusses more in detail the effect of solvent used and additives on the nanomorphology of OSC.

2.5.1 Effects of Processing Solvent

Solution processed films are proving to be more advantageous than other film processing techniques due to the ease of use of its equipment, low cost and lesser time requirement[80]. Hence, it is the methodology of choice when fabricating organic optoelectronic devices, another reason for this is that it allows freedom of manipulation of the morphology of the film formed. This then means that the solvent used to dissolve the donor and acceptor material play a very critical role in the formation of the film as it sets the tone for how the film is formed and the final morphology of the film. The final film morphology is often dictated by the properties of the solvent such as boiling point, vapour pressure, solubility and polarity. The impact of solvent on device efficiency was demonstrated in 2001 by Shaheen et al. for the poly-[2-(3,7-dimethyloctyloxy)-5-methyloxy]-para-phenylene-vinylene(MDMO-PPV):[6,6]-phenyl-C_{61}-butyric acid methyl ester (PCBM) blend system. The strong dependence of device performance on the solvent was shown by the authors by changing the solvent from toluene to chlorobenzene (CB) the PCE improved from 0.9% to 2.5%, also increases of over two folds were seen in the short

circuit current density [55]. Liu et al. researched the correlation between the solar cell device parameters poly(2-methoxy-5-(2'-ethoyl-hexyloxy)-1,4-phenylene vinylene (MEH-PPV): C_{60} with different solvents (xylene, chlorobenzene, 1,2-dichlorobenzene, chloroform and tetrahydrofuran). The authors claimed that non-aromatic solvents prevent intimate contact between the MEH-PPV backbone and C_{60}, thus reducing the charge transfer efficiency and subsequently the photocurrent, but increasing the photovoltage. Also, atomic force microscopy (AFM) measurements revealed that tetrahydrofuran (THF) based devices exhibited a larger scale of phase separation [83]. The use of host solvents is crucial to optimizing device performance. As described above, the choice of host solvent or solvents not only influences domain size and shape but also determines vertical material distributions and the degree of crystallinity in the active layer materials, commonly used solvents for solution processed organic solar cells are given in Table 2.1.

Table 2.1 Common organic solvents used for OSC processing and their properties

Solvent	Formula	MW	Boiling point (°C)	Melting point (°C)	Density (g/mL)	Chemical Structure
1-butanol	$C_4H_{10}O$	74.12	117.7	-88.6	0.8095	
2-butanol	$C_4H_{10}O$	74.12	99.5	-88.5	0.8063	
chlorobenzene	C_6H_5Cl	112.56	131.7	-45.3	1.1058	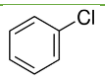
chloroform	$CHCl_3$	119.38	61.2	-63.4	1.4788	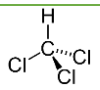
1-propanol	C_3H_8O	88.15	97	-126	0.803	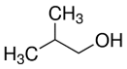
2-propanol	C_3H_8O	88.15	82.4	-88.5	0.785	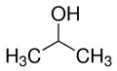
tetrahydrofuran (THF)	C_4H_8O	72.106	65	-108.4	0.8833	
toluene	C_7H_8	92.14	110.6	-93	0.867	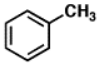
o-xylene	C_8H_{10}	106.17	144	-25.2	0.897	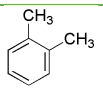
m-xylene	C_8H_{10}	106.17	139.1	-47.8	0.868	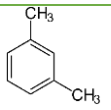

2.5.2 Effect of Solvent Additives

The use of solvent additives has in recent years been gradually adopted as the primary way of influencing the nanoscale morphology of the active layer during spin casting [76]. The

solvent additives help by selectively dissolving one of the components of the active layer material in the base solvent and depending on the additives' boiling point, the left over high boiling point solvent acts as a plasticizer to reduce the Tg of the film and allows for a diffusion and phase separation at lower temperature than normally possible, this is also why it is so important to get rid of the high boiling point solvents after processing, long enough to form a good morphological blend. The first instance for the use of solvent additives was in a PCPDTBT:PCBM system, where an addition of a small amount of 1,8-octanedithiol (ODT), yielded a PCE increase from 2.8% to 5.5% through significantly improved morphology [60]. Also, the effects of 1,8-diiodooctane (DIO) as an additive to PTB7:$PC_{71}BM$ OSCs was studied by the group of Chen. The study revealed that without DIO, the large PCBM aggregates prevented intermixing of PCBM into PTB7 domains. DIO dissolved the PCBM aggregates and resulted in smaller domains with improved PTB7:PCBM interpenetration network, the relative effect of the additive on the domain size is seen in figure [84].

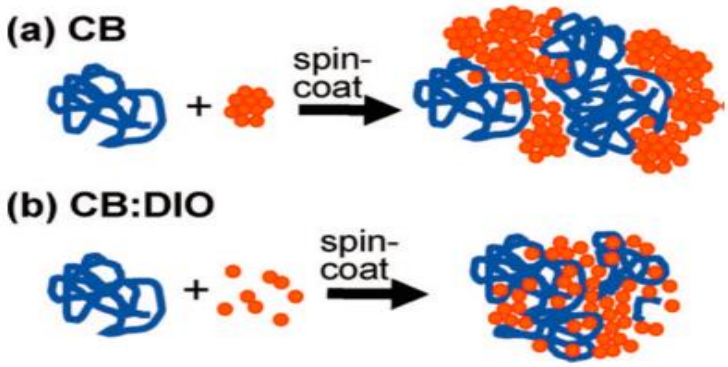

Figure 2.12 Schematic of PTB7 and $PC_{71}BM$ aggregation in (a) CB and (b) CB: DIO with the resulting film morphology*[84]*.

3 Materials and Methods

In this chapter details of the experimental process are describe and this includes; physical and chemical properties of materials investigated, device and sample preparation, characterization techniques as well as data analysis methods.

3.1 Materials

The inherent drawbacks of fullerene acceptors, such as the difficulty of tuning energy levels, poor visible light absorption, and its ease of aggregation, make it difficult to further improve photovoltaic performance of the PSC. This has led to the synthesis of acceptors that can overcome such barriers as stated earlier. Among the non-fullerene acceptors, a variety of n-type conjugated polymers with strong electron deficient groups, like in aromatic diimide (such as perylene diimide, naphthalene diimide, and naphthodithiophene diimide), are explored as polymer acceptors. Also, n-type organic semiconductors (n-OSs) having an A−D−A (acceptor−donor−acceptor) structure like diketopyrrolopyrrole- based n-OSs have been successfully employed in PSC. The use of Low bandgap A−D−A structured n-OSs has piqued the interest of researchers for its ability to harvest light in the visible-near infrared range and as such can improve the efficiency of PSC [85]. The materials used for this study can be group according to their layer stack positioning and are discussed below.

3.1.1 Active layer Materials

For fabrication of the solar cell, the active layer deposition two different configuration was used, first with the donor and a fullerene acceptor as reference devices, second was based on a non-fullerene acceptor as the material of study. The donor material is a side chain based statistical copolymer with random distribution of segments of linear octyloxy side chains and of branched 2-ethylhexyloxy side chains on an anthcene-containing poly (p-phenylene-ethynylene)-alt-poly(p-phenylene-vinylene) (PPE-PPV) backbone known as AnE-PVstat polymer. The synthesis of this polymer was described in detail in [86] the fullerene acceptor used is a derivative of C_{60} known as phenyl C_{61} butyric acid methyl

ester (PCBM) while the non-fullerene acceptor is a novel material based on bulky seven-ring fused core (indacenodithieno [3,2-b]thiophene, IT), end-capped with 2-(3-oxo-2,3-dihydroinden-1-ylidene)malononitrile (INCN) groups, and with four 4-hexylphenyl groups substituted on it. From the original publication on the synthesis of ITIC, it is reported to have strong and broad absorption, low LUMO and HOMO energy levels, good electron transport ability, and good miscibility with polymer donors, the synthesis of this material is also given in detail in the same work [87]. Also three non-fullerene acceptors derived from Perylene Diimide (PDI) dimers were investigated; the first PDI_2AC_2 was synthesized by connecting two PDI monomers with a double acetylene bridge. The second – DPP-$(ac\text{-}PDI)_2$ is obtained by a synthesis of Diketopyrrolopyrrole (DPP) connected to the two molecules of PDI with two acetylene bridges on either side. DPP based materials have been so far investigated for its good charge carrier mobility and fluorescent properties. The third was based on thienoisoindigo (TII) and acetylene as the link between the PDI dimer, based on earlier research molecules derived from thienoisoindigo have shown good optical properties and charge carrier mobilities but have not been investigated properly in OSC applications. The schematic of all materials used for this study are given in Figure 3.1 and Figure 3.2. However, as a first step other non-fullerene acceptor were investigated using cyclic voltammetry for their compatibility with the acceptor material.

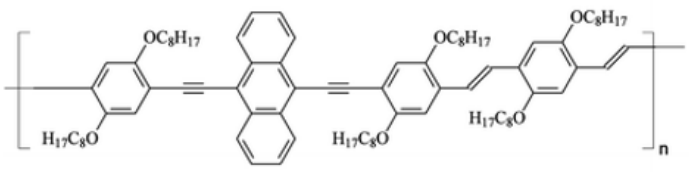

AnE-PV*stat*

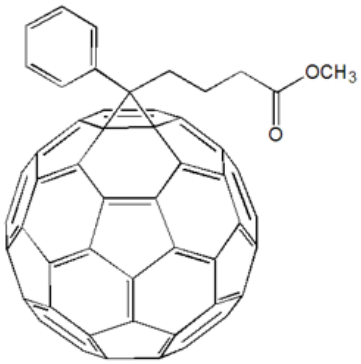

$PC_{61}BM$

Figure 3.1 Donor Material AnE-PVstat and Fullerene acceptor PCBM

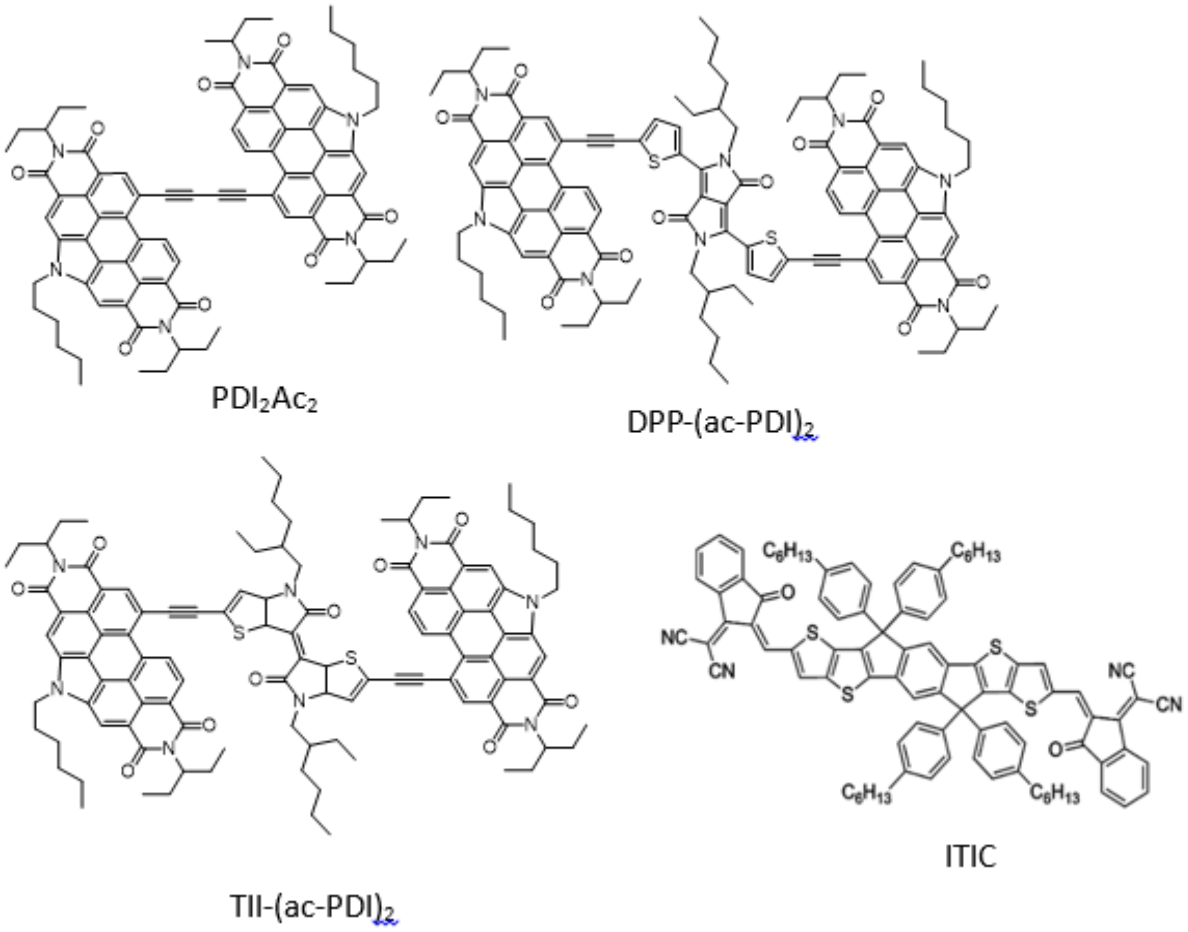

Figure 3.2 Chemical structures of Non-Fullerene acceptors ITIC, PDI_2AC_2, $DPP\text{-}(ac\text{-}PDI)_2$, TII-(ac-PDI)2

3.1.2 Transport Layer Materials

PEDOT:PSS was used as the HTL for fabrication of devices in standard geometry, due to its high work function (matching the HOMO level of commonly used donor polymers well), high transparency in the visible range (higher than 80%), good electrical conductivity and the ability to reduce the ITO surface roughness, while increasing its work function [88]. However, PEDOT:PSS is highly hydrophilic; thus, bad film morphology and worse electrical properties have been observed when deposited as the HTL onto the hydrophobic organic layers in inverted devices. Hence for the inverted geometry MoO_3 was used. MoO3 has been reported to increase the overall efficiency of a BHJ inverted solar cell, the result was based on both a P3HT:PCBM active layer and a nanocrystalline

TiO_2 ETL [88]. For the inverted device layers of polyethylenimine (PEI) and Titanium Oxide were deposited sequentially as the ETLs. The major kick for ETLs is the requirement of high transparency, TiOx, has attracted great attention in ISCs, largely due to their excellent optical transmittance, high refractive index and good chemical stability. Further use of a combination of TiOx /PEI layer has been shown to possess high transparency, improved electron mobility, reduced series resistance and increased electron extraction at the cathode interface [89].

3.1.3 Electrode Materials

The top electrode in both the inverted and standard geometry was indium tin oxide (ITO) while the bottom electrode for the standard and inverted were aluminum and silver respectively.

3.2 Sample Preparation

The samples used for the purpose of this thesis includes thin films for optical measurements and solar cell devices for electrical characterization.

3.2.1 Solution Preparation

The organic materials were obtained in solid form and made into solution using a solvent mixture of chlorobenzene and chloroform in 1:1 ratio, as the polymer material is found to be very soluble in the combination. The solution concentration chosen for this work is between 12 – 18 mg/ml for the different materials, the values were chosen from internally optimized parameters.

Table 3.1 Summary of Concentration of materials in blend

Donor-Acceptor Interface	Blend ratio
AnE-PVstat/ITIC	1:1
AnE-PVstat/ PDI_2AC_2	2:3
AnE-PVstat/DPP-(-acPDI$_2$)	2:3
AnE-PVstat/TII-(-acPDI$_2$)	2:3
AnE-PVstat/PCBM	2:3

3.2.2 Films

The films were prepared by spin coating at 600 rpm for 45 seconds on pure glass substrates. The substrates for film deposition were prepared by cleaning first with tips dipped in acetone and then subsequent cleaning with ultrasonic bath using acetone and isopropanol for 15 minutes each. The films used for UV-Vis spectroscopy were also used for photoluminescence measurements.

3.2.3 Solar Cell Devices

For solar cell device preparation glass substrates of 25.3 x 25.3 x 1 mm substrates with etched ITO coating (150nm) purchased from Kintec Corporation were used. The substrates were cleaned in the same way as the glass substrates for film deposition. The two device architectures were built using the conventional device as reference for tests carried out on the inverted structures. PSC devices with a structure of ITO/PEDOT:PSS/AnE-PVstat:Acceptor/Al (conventional) fabricated as follows and measured using the Keithley 2400 Source/Measure Unit and measured under the AM 1.5G spectrum at a calibrated light intensity of 100 mW/cm^2. The clean indium tin oxide (ITO)-coated glass substrate with sheet resistance of 10 Ω/square was used as the substrate after ultrasonic treatment. PEDOT: PSS (Clevious PH) layer was spin casted onto the ITO substrate at 3500 rpm for 35 secs and then annealed at 150 °C for 15 minutes. The active layer consist of AnE-PVstat and ITIC was casted directly from CB : CF (1:1) solution onto the PEDOT:PSS layer by spin coating. After which 100 nm Al was successively deposited onto the active layers under high vacuum. The Inverted devices were fabricated with a geometry of ITO/PEI/TIOx/AnE-PVstat:ITIC/MoO_3/Ag. The PEI (0.27mg/ml in butanol) layer was spin cast at 2000 rpm for 30secs and annealed in the glovebox under nitrogen condition for 105 ^{0}C for 5 minutes, this was closely followed by the deposition of TiO_x (1.5 Vol% in Isopropanol) also at 2000rpm for 30secs and annealed in air for 110 ^{0}C for 10minutes. After which the different active layers were deposited and 10nm of MoO_3 and 100nm of Ag were evaporated under vacuum pressure (2.7 x 10^{-6} bars). The devices were encapsulated using glass substrates with epoxy resin under a laser beam in a controlled nitrogen environment

(O_2 value of 10ppm and H_2O value of 0.3 ppm). The total cell area obtained was 0.42 cm^2 and a total of 8 cells were fabricated per parameter.

3.3 Characterization Methods

The characterization methods applied in this work could broadly be classified into 3; electrochemical characterization, Optical characterization and Electrical characterization.

3.3.1 Cyclic Voltammetry (CV) Measurement

This is an electrochemical method used for evaluation of the position of HOMO and LUMO energy levels and the band gap of the polymers. It is also useful for investigating reversibility, stability and rearrangements of the polymer films deposited on the electrode. In principle, one can obtain the redox properties, information on the oxidation and reduction potentials of organic materials from the cyclic voltammetry. The oxidation corresponds to electron extraction from the HOMO level and can be correlated to the ionization potential, whereas the reduction potential is associated with electron affinity and indicates the LUMO level. In CV measurements, a continuously varied voltage is applied (linear sweep) while the current is measured. The input parameters are therefore the initial and final voltage and the scan rate, while the output parameters are the voltages values at which the peaks occur and current intensities. The CV measurements for this work were made in chloroform containing 0.1 M tetrabutylammonium hexafluorophosphate (Bu_4NPF_6) at a scan rate of 200 mV/s performed. The potentials are given relative to the ferrocenium / ferrocene redox couple. The redox potential for the ferrocenium / ferrocene redox couple is taken as 5 V as reported in [90], where the redox potentials of the couple were calculated for most common non-aqueous solutions. From the results obtained, the potentials of the onset of the first oxidation and first reduction of a material can be correlated to the energies of its highest occupied molecular orbital (HOMO) and lowest unoccupied molecular orbital (LUMO), respectively. This is done by taking intersection of the tangents between the baseline and the signal current as depicted in Figure 3.3.

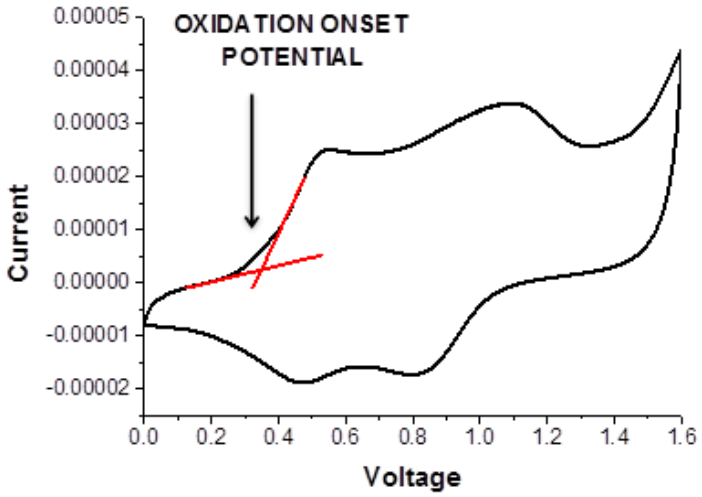

Figure 3.3 Depiction of CV diagram and the method of extracting the oxidation onset potential *[91].*

The HOMO and LUMO levels are then correlated using equation 3.1 and 3.2

$$E_{HOMO} = -((E_{ox})_{onset} + 5)\ \text{eV} \tag{3.1}$$

$$E_{LUMO} = -((E_{red})_{onset} + 5)\ \text{eV} \tag{3.2}$$

3.3.2 UV-Vis Spectroscopy

This technique is applied for measuring the spectral absorption distribution of the spin coated films in the wavelength range from near ultraviolet (190-400nm) to visible light (400-90nm). UV-Vis can be applied to distinguish changes in the electronic transitions of the molecules. For this work the absorption data was obtained simply by shining monochromatic light on the sample film and recording the transmitted light and reflected light. After which the absorption is calculated from equation 3.1.

$$A = 100 - (R + T) \tag{3.3}$$

Where, A is the absorption in %, R is the reflection and T is the Transmission of the deposited film.

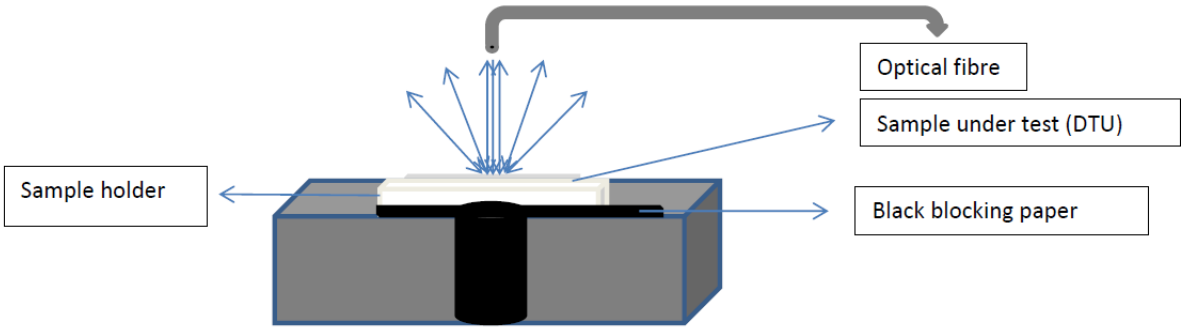

Figure 3.4 Measurement setup for UV-Vis Spectroscopy

The sample was deposited on a pure glass substrate. From the absorption measurements, one can roughly estimate the optical bandgap of the absorbing semiconductor, conjugation length- a longer conjugation length is indicated by longer wavelength of the absorption peak. The absorption spectrum measurements can also help in recording morphology changes (such as crystallinity of the polymer) in the materials or blends during device processing. The setup for the measurement is given in Figure 3.4, the instruments are first calibrated for maximum transmission in air and maximum reflection using an aluminum glass mirror. The data obtained is saved as a reference for all the measured data.

3.3.3 Photoluminescence (PL) spectroscopy

This is a contactless, nondestructive method of probing the structure of materials. Light is directed onto a sample, where it is absorbed and imparts excess energy into the material. One way this excess energy can be dissipated by the sample is through laminating effect (emission of light). In this case the luminescence is called photoluminescence because the material is excited by a photo excitation process. This technique can be used for defining the effectiveness of the excited charge separation at the interface between donor and acceptor. When the polymer material is shined with light, the polymer emits light through the photoluminescence process. When an acceptor material is added in the mixture a quenching of photoluminescence takes place, since some of the excitons are separated at

the interface and the radiative recombination is reduced. When a complete quenching is achieved it indicates that all the excited pairs are successfully separated to free carriers. Pl is used as a means of testing polymer blends by the utilization of the dependence of the photophysical process of intermolecular energy transfer and excimer formation. PL spectrum can be used for studies on charge transfer states and polymer degradation, as much as the use of PL is very important in determining the dissociation of excitons, it does not give a holistic view as there could be other processes such as non-radiative recombination responsible for the quenched blend luminescence. In this thesis, steady state PL spectra was recorded using an Avantes avaspec 2048 fiber spectrometer over a wavelength between 500 and 1100 nm at using a laser at 405 nm. The obtained values were normalized to the absorption value at the laser excitation.

3.3.4 IV curve and EQE Measurement

This method is used to check the device performance based on the diode characteristics of the solar cell. Values such as V_{oc}, J_{sc}, FF, PCE, R_{sh}, R_p can be then extracted from the measured IV curves when the device is placed under illumination, which are the most important parameters that define the device performance as discussed in section 1.3. While taking the device characteristics under A.M 1.5G illumination (Figure 3.5) of a xenon arc lamp calibrated to 100mW/cm^2 it is equally important to get the dark measurement. The dark is taken by covering the device from any form of illumination and applying a varying voltage usually from +2 to -2V same as is done under illumination. The dark measurement gives extracting information about series resistance, shunt resistance, saturation currents and ideality factors.

Another important parameter that could be measured to give a more accurate and precise result for the J_{sc} is the external quantum efficiency (EQE). This is the ratio of the number of charge carriers collected by the solar cell to the number of photons of a given energy shining on the solar cell from outside (incident photons). EQE gives information whether the absorbed photons are being efficiently converted to charge carriers and collected at the

electrodes. Systems with different operational mechanisms have been developed for measuring the EQE but it generally involves using a monochromatic light with a known intensity and measuring the current while changing the wavelength along the absorption spectrum of the device.

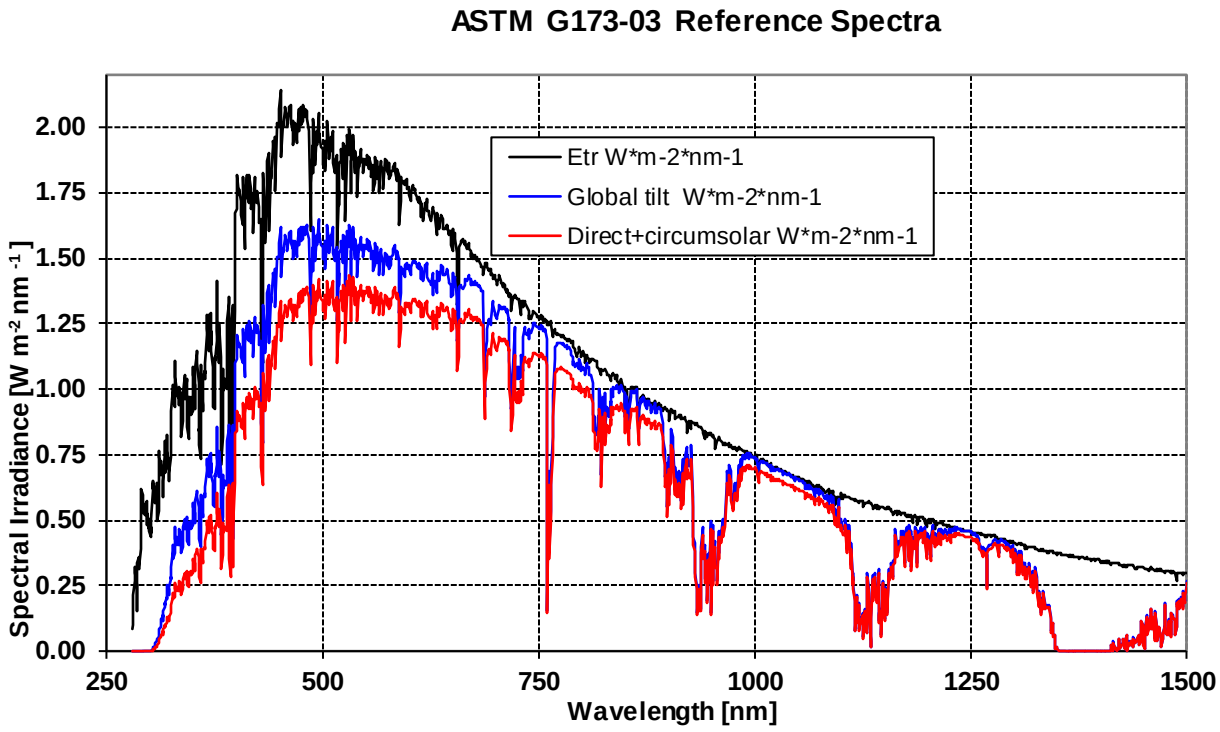

Figure 3.5: Reference spectral Irradiance [92]

4 RESULTS AND DISCUSSION

In this chapter results from the various characterization processes are presented and discussed. These results will be compared to results from existing literature and inferences would be drawn from theoretical backgrounds. First the results from cyclic voltammetry are shown with an indication of a possible formation of a type II heterojunction, followed by results from optical measurements and then device characterization based on materials that were deemed compatible.

4.1 Investigation of Interfacial Energy Level Alignment

The energy level alignment is very critical when possibility of charge separation and transfer in heterojunction solar cells are being visualized. The knowledge of this alignment comes from the depiction of the energy bands of the material systems being investigated. In principle there are three types of band alignment at interfaces of semiconductor materials; type I (straddling gap), type II (staggered gap) or type III (broken gap). For photogenerated excitons in both materials to dissociate and separate for onward transport to the two electrodes, the energy level of the materials need to form a type II heterojunction [93]. Also, these energy levels and their arrangements are crucial for generating photovoltage (V_{oc}), the V_{oc} is largely dependent on the energy offset at donor/acceptor interfaces. Since there exists a minimum energy offset required for efficient exciton dissociation or charge transfer, the V_{oc} could be largely lowered by too large energy offsets. In order to determine the energy levels of the materials being investigated 5 mg of each pristine material was taken and processed as described in section 3.3.1 for cyclic voltammetry characterization. The results obtained are given as a comparison between each no-fullerene acceptor and the donor (AnE-PVstat).

4.1.1 Energy Offset

From the measured data obtained in CV (Figure 4.1), the material combinations all form a staggered heterojunction (type II) Figure 4.2. However as stated in [19] where empirical relations of LUMO energy offsets (ΔE_{LUMO}) to power conversion efficiencies were given,

the minimum ΔE_{LUMO} required for efficient charge dissociation is stated to be 0.3 eV. This necessitates further quantification of the energy offset of each D – A pair as a possible indication of their probability to overcome the columbic binding forces. Hence, ΔE_{LUMO} for each material system was calculated based on equation 4.1

$$\Delta E_{LUMO} = E_{LUMO}^{Donor} - E_{LUMO}^{Acceptor} \quad (4.1)$$

Where, E_{LUMO}^{Donor} is the LUMO energy level for the donor and $E_{LUMO}^{Acceptor}$ is the LUMO energy level for the acceptor. The values for each is obtained from the energy level diagrams given in Figure 4.2.

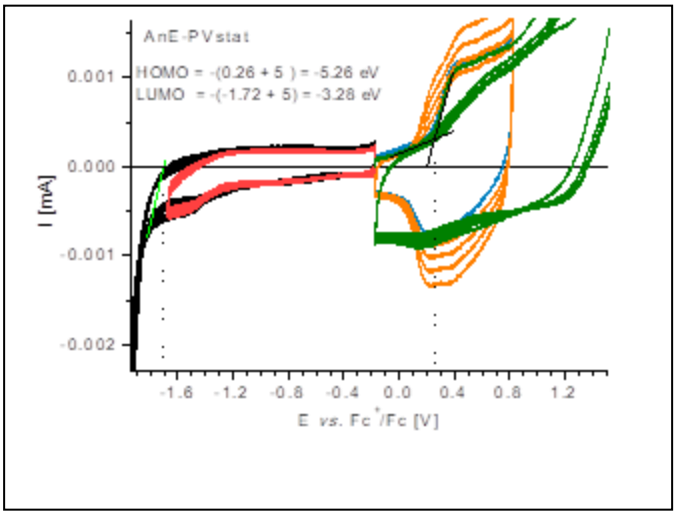

(a

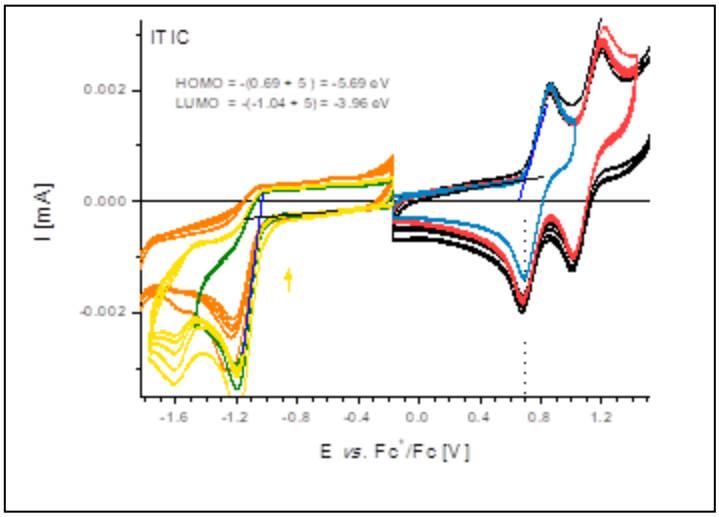

(b

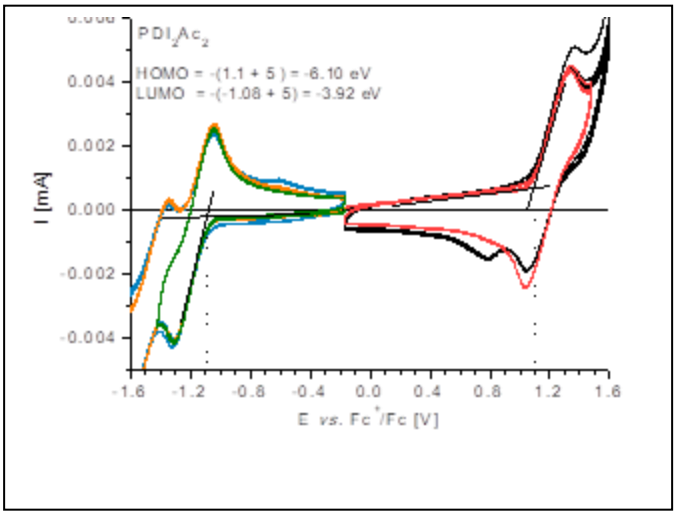

(c

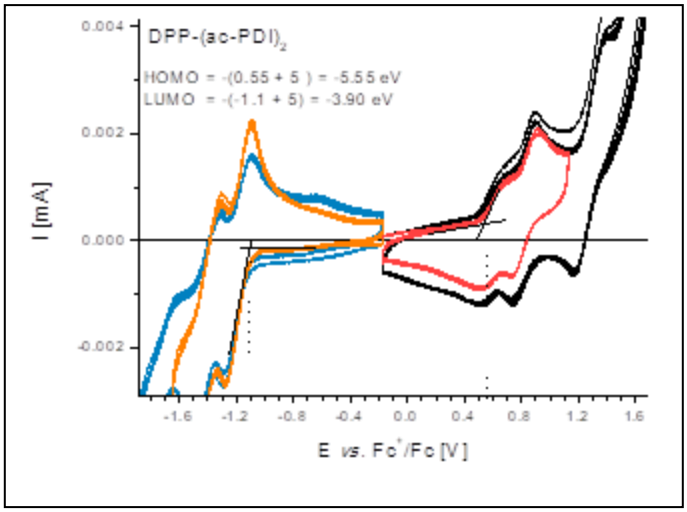

(d

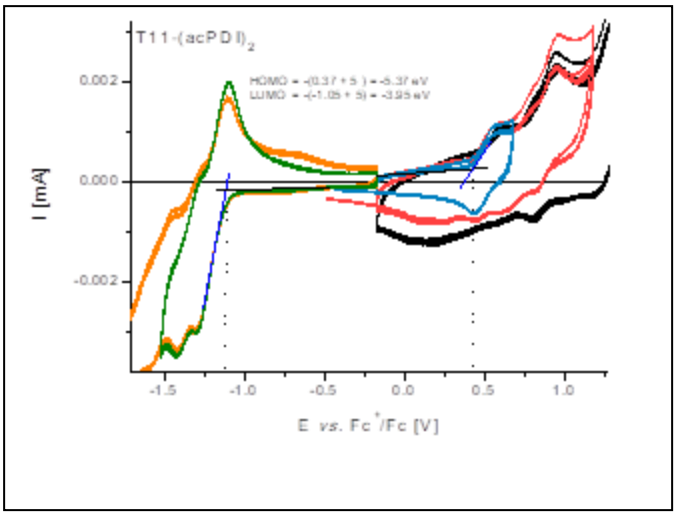

(e

Figure 4.1: Graphical results from cyclic voltammetry analysis of (a) AnE-PVstat (b) ITIC (c) PDI_2AC_2 (d) DPP-(-acPDI$_2$) (e) TII-(-acPDI$_2$)

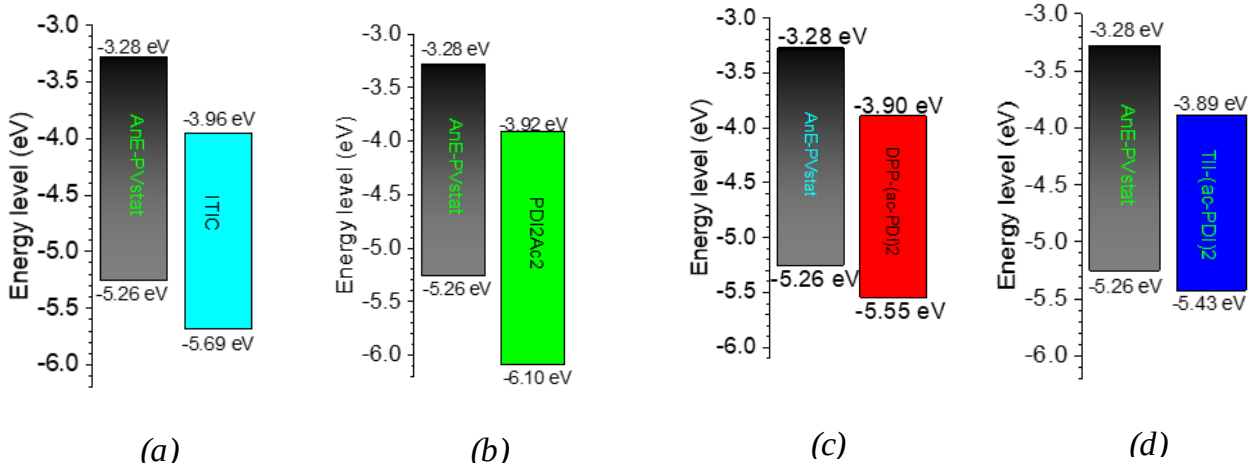

Figure 4.2 Schematic of the LUMO and HOMO energy levels calculated from CV results for Donor (AnE-PVstat) and acceptors a) ITIC b) PDI_2AC_2 (c) DPP-(-acPDI$_2$) (d) TII-(-acPDI$_2$)

The calculated values for ΔE_{LUMO} , ΔE_{HOMO} as well as the effective interfacial gap (E_{DA}) are presented in Table 4.1, where

$$\Delta E_{HOMO} = E_{HOMO}^{Donor} - E_{HOMO}^{Acceptor} \quad (4.2)$$

$$E_{DA} = E_{LUMO}^{Acceptor} - E_{HOMO}^{Donor} \quad (4.3)$$

Table 4.1 Calculated energy offsets for the different donor/acceptor interfaces investigated

Donor-Acceptor Interface	ΔE_{LUMO} (eV)	ΔE_{HOMO} (eV)	E_{DA} (eV)
AnE-PVstat/ITIC	0.68	0.43	1.3
AnE-PVstat/ PDI_2AC_2	0.64	0.84	1.34
AnE-PVstat/DPP-(-acPDI$_2$)	0.62	0.29	1.36
AnE-PVstat/TII-(-acPDI$_2$)	0.61	0.17	1.35

From the values obtained in Table 4.1 for ΔE_{LUMO} and ΔE_{HOMO} an inference can be made of charge dissociation capabilities of the donor - acceptor pair based on Marcus theory [19]. However, further studies carried out by Rand and Burk [94] indicate an increase of electron transfer rates with the offset energies implying that the pairs of AnE-PVstat with ITIC and PDI_2Ac_2 are likely to have higher electron transfer rates.

4.2 Optical properties

The absorption properties of the materials were investigated as described and the values calculated from measured reflection and transmission data. The results are presented in Figure 4.3, the pristine donor has an absorption onset around 620 nm (2 eV), this value is comparable to that obtained in the original work [86] and that obtained for the electrochemical analysis. This is an indication that the bandgap of the donor is approximately 2 eV with an absorption peak around 520 nm. As seen from the absorption spectra, PCBM has nearly no absorption in the UV-Vis range and pulls the absorbance of the donor down in the resulting blend Figure 4.3a.

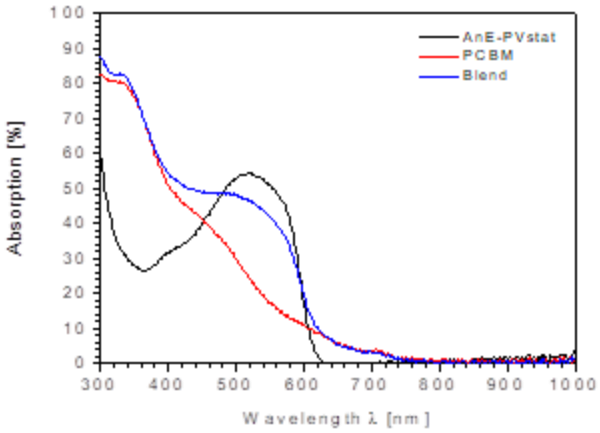

(a)

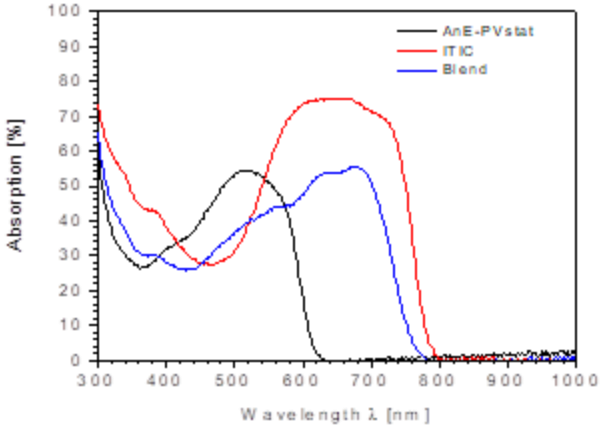

(b)

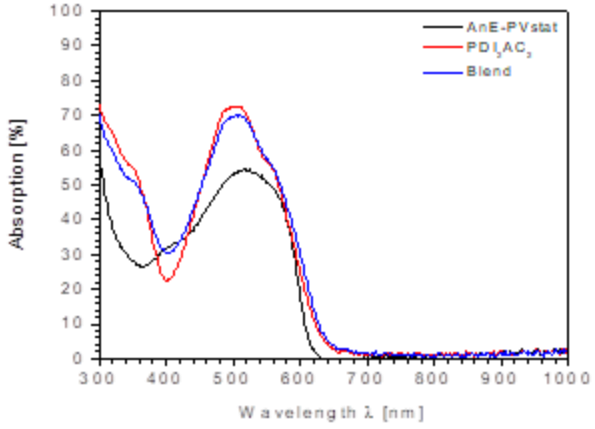

(c)

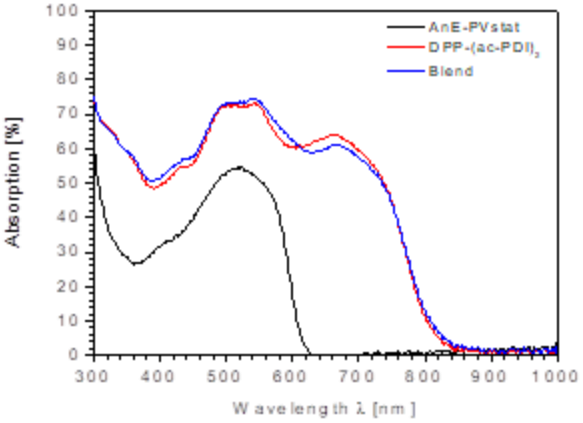

(d)

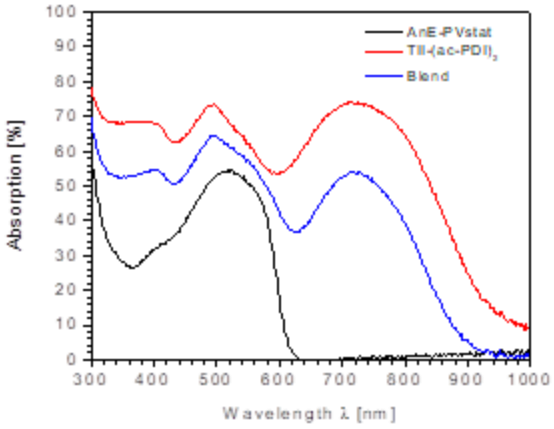

(e)

Figure 4.3 Graphical results from absorption analysis of pristine and blends with (a) PCBM (b) ITIC (c) PDI2AC2 (d) DPP-(-acPDI2) (e) TII-(-acPDI2)

Unlike pristine ITIC which has an almost complementary absorption spectra leading to a widening of the absorption range of the blend and a red shift in the absorption peak of the donor. The non-fullerene acceptors derived from the PDI dimers show a slightly different behavior; PDI_2AC_2 has an absorption spectra that is almost similar to that of AnE-PVstat and its absorption has little impact on the final absorption of the blend. The other two acceptors show an absorption over the full range of the UV-Vis region which also leads to an increased possibility of collection of photons.

Photoluminescence measurement also show a large degree of quenching for all material combinations. This is an indication that the photons absorbed by the active layers lead to an efficient generation of electron-hole pairs. It could also be seen from the blend with ITIC that there is some remnant luminescence which results from the acceptor material. Also, it is seen from the ITIC blend spectra that the quenching of the donor could be as a result of finely molecularly intermixed phases with ITIC, leading to too small phase separation for charge transport. However, for the case of the PDI derived acceptor materials the PL spectra shows incomplete quenching of the donor signal for TII-$(ac\text{-}PDI)_2$ blend, while the others show complete quenching. Also the PCBM blends are completely quenched as seen from Figure 4.4a. The complete graphical depiction of the PL spectra for the different pristine materials and blends is shown in Figure 4.4. The PL intensity of DPP-$(ac\text{-}PDI)_2$ is increased in the blend in comparison to the pure film and a similar case is observed for TII-$(ac\text{-}PDI)_2$. This is opposed to the strong quenching of the PL signal upon observed for PDI_2 and PDI_2Ac_2 which suggest a suitable alignment for a working solar cell.

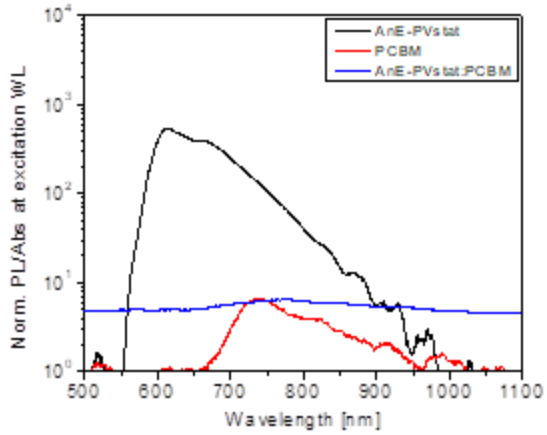

(a)

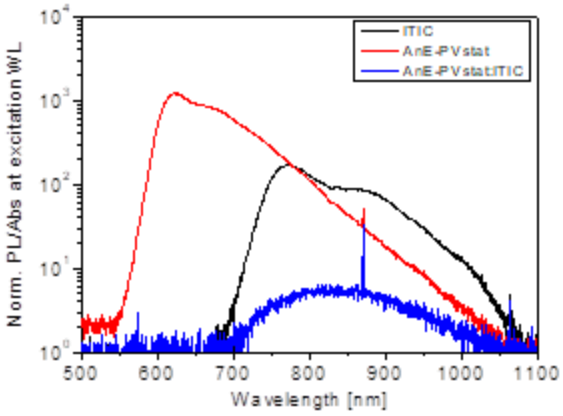

(b)

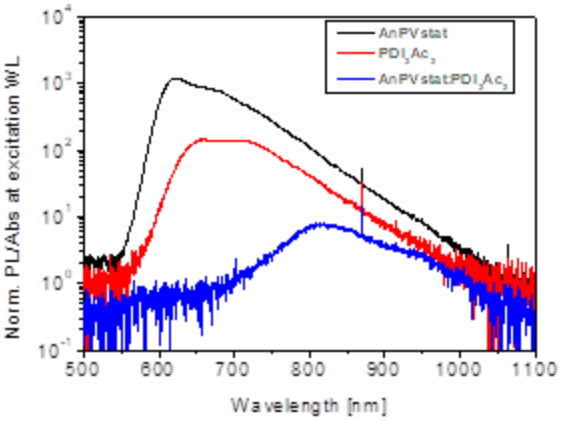

(c)

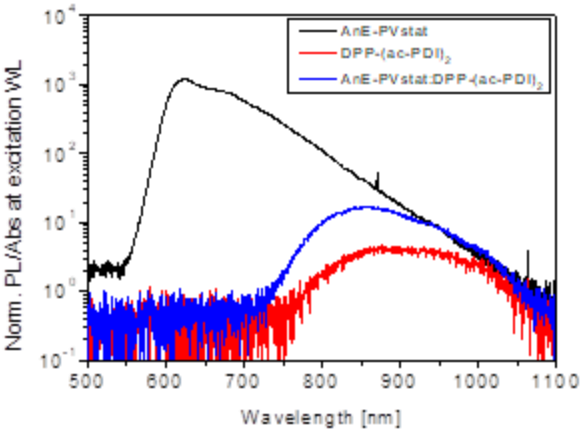

(d)

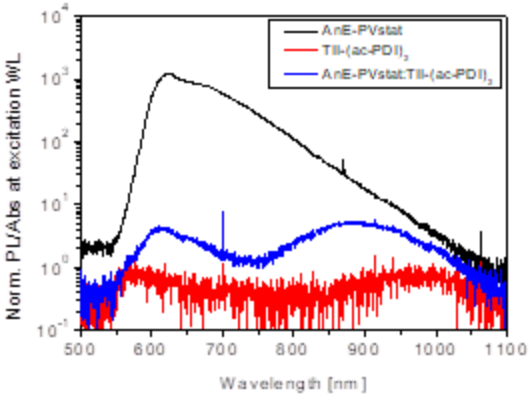

(e)

Figure 4.4 Photoluminescence measurement of Pristine and Blend Films

4.3 Solar cell device performance

ITIC as a non-fullerene acceptor is setting itself as an acceptor of reference for OSC built from non-fullerene acceptors since its first report, devices built from the acceptor material has shown record efficiencies and photovoltaic characteristics, based on this only devices fabricated from ITIC and PCBM are detailed in this work. However, the other material combinations were investigated and results (with I-V curves) are given in the appendix.

Table 4.2: Best Cell Device Parameters

Donor	Acceptor	Device Configuration	Jsc (mA/cm²)	Jsc corrected (mA/cm²)	Voc (mV)	FF (%)	PCE(%) corrected	PCE (%)
AnE-PVstat	ITIC	Conventional	1.972	1.436	836	30	0.360	0.49
AnE-PVstat	ITIC	Inverted	2.58	1.686	978	32	0.528	0.8
AnE-PVstat	PCBM	Conventional	5.55	3.521	854	56	1.684	2.65
AnE-PVstat	PCBM	Inverted	4.872	3.989	814	48	1.559	1.89
AnE-PVstat	DPP-(ac-PDI)$_2$	Inverted	0.034	0.039	954	33	0.012	0.01
AnE-PVstat	PDI$_2$Ac$_2$	Inverted	0.388	0.366	1067	29	0.113	0.12
AnE-PVstat	TII-(ac-PDI)$_2$	Inverted	0.01	0.020	833	37	0.006	0

The results for the best cells from all the cells investigated are presented with ITIC having a higher PCE in inverted structure when compared to the standard device structure unlike PCBM which has a better device performance in standard architectures. The results show a high open circuit voltage of above 1 V (in the case of DPP-(ac-PDI)$_2$). However, the active layers based on PDI dimers have little or no current generation, this could be as a result of a too intimately mixed active layer morphology and a lack of percolation network that allows for generated carriers to get to the interface of the electrode for collection. All devices show very low fill factors of less than 60%. The best PCE is obtained from the device based on PCBM in conventional architecture.

4.3.1 Effect of Anti-Solvent Addition

The effect of Isopropanol on the I-V characteristics was investigated and there is an observed improvement in the short circuit photocurrent in the case of PCBM up to 10%

which is assumed to be related to the limited solubility of PCBM. Also the devices made from ITIC saw an improvement in device parameters up to the maximum value added. The improvement in the performance of the cells is due to the nanoscale morphological separation and aggregation of the donor and acceptor phases also more charges to be extracted hence leading to an increase in the power conversion efficiency. The choice of Isopropanol was based on a study conducted by [95] where ITIC was investigated in combination with custom synthesized polymers and the use of Isopropanol (IPA) led to the achievement of a PCE of 11.34% with a V_{oc} of 0.95 V and also based on the boiling point of IPA which lies between that for chloroform and chlorobenzene. However in our study, we observe a 15% increase in the J_{sc} for devices fabricated with 30 Vol% of IPA in the donor for ITIC while for PCBM there was an increase of 50% in the J_{sc}. The results for the different variations of IPA additions are presented in Table 4.3. In Figure 4.5 we see the behavior of these devices under illumination and it is observed that the blends with PCBM show good diode characteristics unlike the devices based on ITIC which show a linear behavior in the reverse direction.

Table 4.3 Summary of parameters extracted from J–V and EQE characteristics of AnE-PVstat:ITIC and AnE-PVstat:PCBM based devices with IPA

Donor	Acceptor	Device Configuration	Isopropanol Amount Vol%	Jsc (mA/cm²)	Jsc corrected* (mA/cm²)	Voc (mV)	FF (%)	PCE(%) corrected*	PCE (%)
AnE-PVstat	ITIC	Inverted	0	2.58	1.686	978	32	0.528	0.8
AnE-PVstat	ITIC	Inverted	3	2.544	2.049	980	31	0.623	0.76
AnE-PVstat	ITIC	Inverted	10	2.94	2.555	983	30	0.753	0.88
AnE-PVstat	ITIC	Inverted	30	2.979	2.623	962	31	0.782	0.89
AnE-PVstat	PCBM	Inverted	0	4.872	3.989	814	48	1.559	1.89
AnE-PVstat	PCBM	Inverted	3	3.425	3.217	823	55	1.456	1.56
AnE-PVstat	PCBM	Inverted	10	6.629	5.703	807	41	1.887	2.2
AnE-PVstat	PCBM	Inverted	30	4.657	3.732	797	45	1.338	1.69

* indicate values corrected by EQE measurement

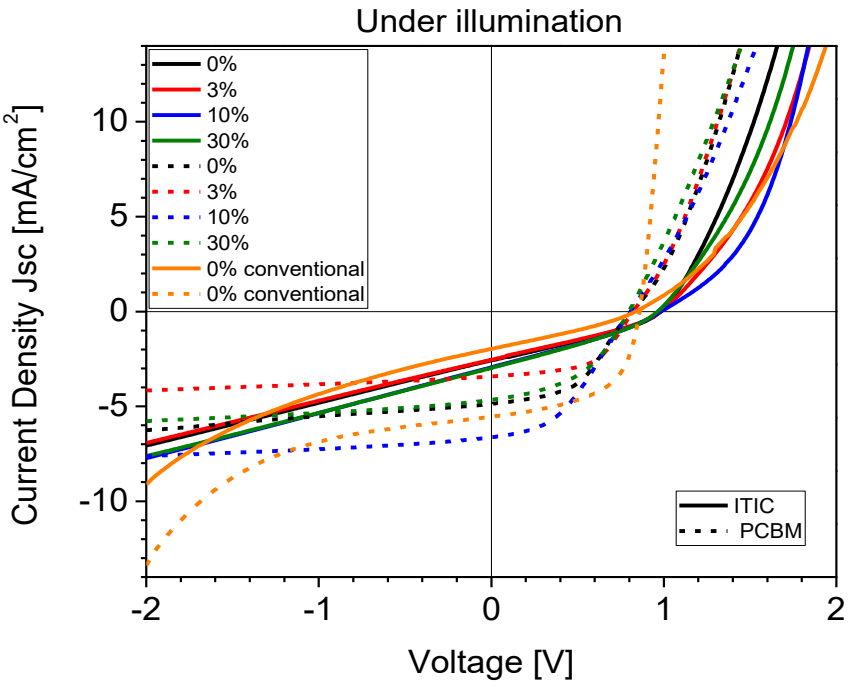

Figure 4.5: J-V characteristics of devices under illumination

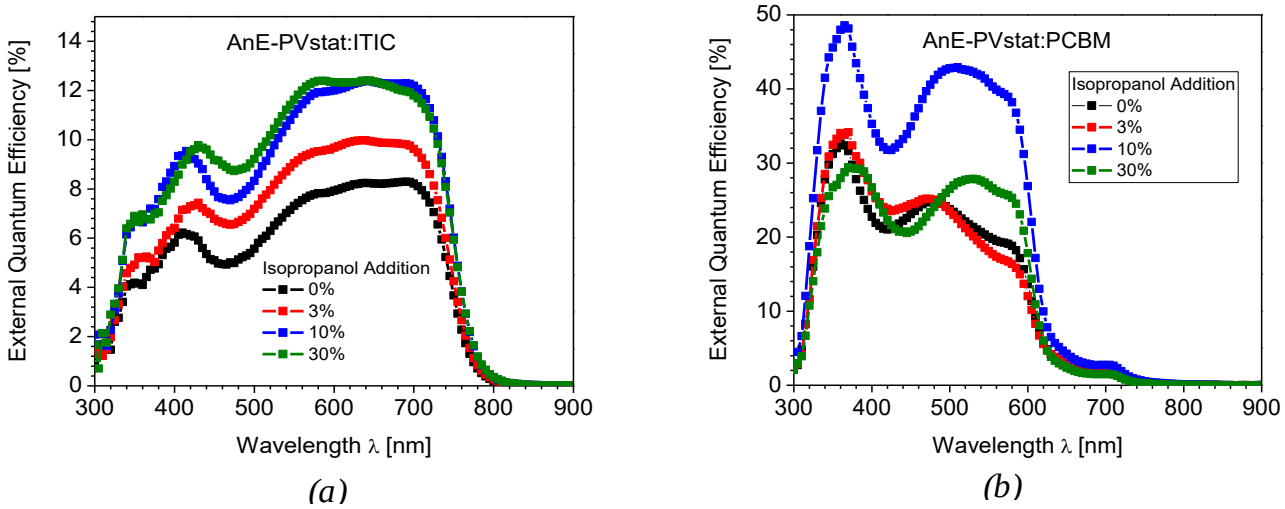

Figure 4.6: EQE characteristics of devices based a) AnE-PVstat:ITIC b) AnE-PVstat:PCBM

4.3.2 Determination of Charge extraction capabilities

The quantum efficiency is measured to accurately depict the spectral response of the devices (Figure 4.6). PCBM based devices have a higher quantum yield of nearly 50% while the devices based on ITIC show very modest values for EQE. In theory from the

results of the CV the AnE-PVstat and ITIC should ideally be compatible and efficiently generate charge carriers, however the results from the solar cells show otherwise. It is therefore important to conduct a further test to understand the limitation of the devices. From literature solar cells could ideally be limited by the generation capabilities or the extraction capabilities. Hence, to test if the devices were being limited by extraction, higher negative voltages were applied (that is to say a higher voltage in the reverse direction). The photovoltaic performance of the PCBM-based device was very different with that of the ITIC based OSCs. To reveal the differences in charge carrier dynamics of devices, the charge extraction characteristics were studied. Figure 4.7 shows the photocurrent density (J_{ph}) versus the effective voltage (V_{eff}) of devices. J_{ph} is defined as $J_{ph} = J_{Light} - J_d$, where J_{Light} and J_d represent for the photocurrent densities under light illumination and in the dark, respectively. Meanwhile, $V_{eff} = V_0 - V_a$, where V_0 is the voltage when J_{ph} equals zero and V_a is the applied voltage. Since V_{eff} is determined by the internal electric field in the BHJ, influencing the charge carriers transport and extraction. It is observed that the J_{ph} linearly increased with increasing the voltage at a low voltage (V_{eff}) region and then tends to get to a saturation point at sufficiently high voltages for PCBM. However the case for the ITIC based device differs as the curve continues to increase linearly without any saturation point in sight. This is an indication that the charge recombination is minimized for the devices with PCBM but may not be the case for the ITIC devices as the saturation current is not approached, hence the charges generated are not efficiently being collected leading to recombinative losses in the cells.

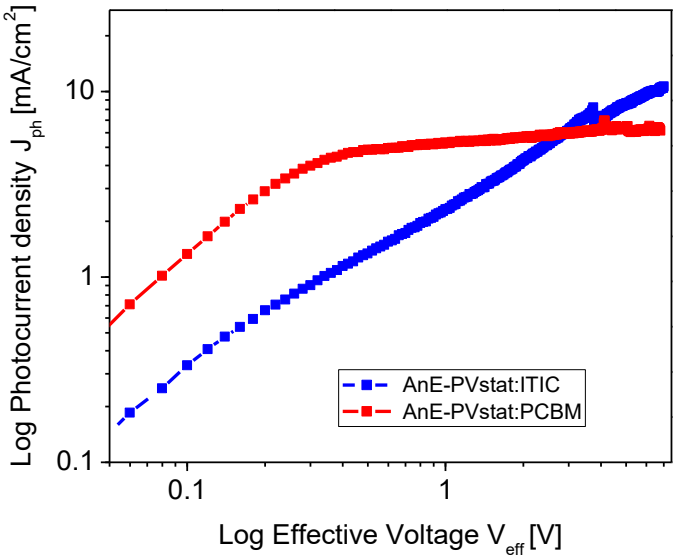

Figure 4.7: Photocurrent density versus Effective voltage characteristics

5 Economics and Application of Organic Solar Cells in Africa

The attraction provided by the use of solar cells that can be adapted to any application provides an incentive for research and development specifically for nations in Africa. As these devices could offer solution to the basic energy requirement for households such as lighting in the most remote locations. It can also be applied for emergency relieve in camps for internally displaced persons or refugees due to its flexibility. In the quest to provide equitable access to energy for all it is important to note that domestic energy need is not limited to households but temporary residents of shelters and camps have to be catered for and as such the benefits of this technology cannot be underestimated. This technology also offers massive reduction in the fabrication process by applying a roll to roll process which is similar to that employed for the mass printing of newspapers. Prototypes are already being tested in Africa to ascertain the suitability of the technology to meet basic requirements, one of which was conducted under the World Bank lighting Africa initiative [96]. The project was based on the replacement of the traditional choice (Kerosene lamps) for solving lighting challenges in remote locations which had several drawbacks such as carbon dioxide emission, fire- and health-hazards. The replacement being a polymer solar cell potentially offers a low cost solution to this problem provided that it could be combined with a storage element and a light source, considering the existence of quite a number of systems that charge batteries but common to all is a too high cost compared to the annual budget of the average user in the sub-Saharan part of Africa. Krebs in this work prepared an ultra-lightweight reading lamp the size of an A4 sheet of paper comprising a polymer solar cell with integrated lithium battery and white light emitting diodes. The industrial manufacture, cost analysis and use of the reading lamp were demonstrated in field tests in Zambia, and it was found that cost of the lamp when manufactured on a small scale was 17.9 € but reductions up to 7€ were attainable by usage of a smaller solar cell. Hence, approaching the required cost of < 3€ corresponding to the typical bi-weekly budget available for lighting purposes [96]. Another demonstration of the practical application of OPVs has been installed at the African Union Peace and Security building which is located

in Addis Ababa (Figure 5.1). Though the economic aspects were not considered, the project forms a unique energy-generating shade sail in the shape of the African continent – which also serves as the logo of the African Union. The active solar shade sail forms the focal point of the new Peace and Security Building of the African Union in Addis Ababa.

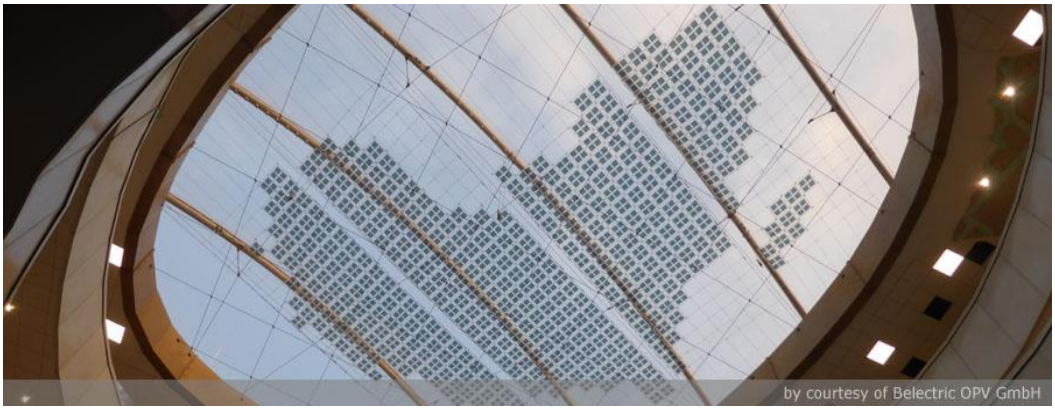

Figure 5.1: OPV installed at the African Union Peace and Security Building

6 Conclusion and Recommendation

In conclusion, a number of novel non-fullerene acceptors were characterized with the donor material AnE-PVstat, a side chain based statistical copolymer with random distribution of segments of linear octyloxy side chains and branched 2-ethylhexyloxy side chains on an anthcene-containing poly (p-phenylene-ethynylene)-alt-poly(p-phenylene-vinylene) (PPE-PPV) using electrochemical methods (cyclic voltammetry), Optical (UV-Vis spectroscopy) and final electrical testing with I-V characterization. It was found through CV that the energy offsets are sufficient enough for charge transfer to occur indicating the presence of a type II heterojunction. Also from optical characterization it is seen that the use of the PDI_2 based electron acceptors improves the absorption range of the active layers unlike in the reference material PCBM. However, electrical characterization in solar cells reveal a very modest performance with the highest PCE for non-fullerene acceptors observed for ITIC at 0.88% with the addition of an antisolvent as against 2.2 % obtained for PCBM. The poor performance could be largely due to the morphological incompatibility of the material which then prevents the extraction of generated charges. It is undeniable that there is an effect induced by the addition of the antisolvent, which serves as good news for the eventual large scale commercialization of OPV. The improvement from the solvent additive is interesting because it eliminates the need for post-production treatments aimed at improving the morphology of the devices, making the manufacturing process easily a continuous one rather than a small batch to batch process considering the large area of cells that would be required for large scale applications. However, for further inference to be made it is important that subsequent tests are carried out such as atomic force microscopy to check the morphology of the active layer, and ultrafast transmission electron microscopy to determine the rate of electron transfer.

For further studies, it is recommended that these novel electron acceptors are tested with polymers with lower bandgaps and that the voltage loss is also calculated to determine the relationship between the photocurrent generation and V_{oc} loss. Another interesting

parameter that could be determined is the probability of extraction of electron to help quantify the percentage of charge that could be extracted from each material system.

Lastly despite the modest values obtained from this research work it is important to note, that OPV research is still at infancy when compared to established silicon technologies and has proven to be a promising field with the rate of improvement of its efficiency. The market that could be occupied by OPV is limitless and not restrictive as the world continues to revolutionize with regards to its energy demand.

References

[1] IEA, "World Energy Outlook," International Energy Agency/ OECD2015.

[2] (20th July). Available: https://www.scientificamerican.com/article/graphic-science-health-care-burden-of-fossil-fuels/

[3] WHO, "Climate change and Health," ed, 2017.

[4] UN. (2015, 12-06-2017). *Sustainable Development Goals*. Available: http://www.un.org/sustainabledevelopment/sustainable-development-goals/

[5] IEA, "Key Renewable Trends Excerpts from Renewables Information " International Energy Agency2016.

[6] IEA, "World Energy Outlook Special Report," International Energy Agency/OECD2014.

[7] UNDP, "Energy and the challenge of sustainability" United Nations Development Programme and World Energy Council2000.

[8] IEA, "Key World Energy Statistics," International Energy Agency2016.

[9] E. Becquerel, "On electric effects under the influence of solar radiation," *Compt. rend.,* vol. 9, p. 561, 1839.

[10] Available: https://sites.google.com/site/mochebiologysite/online-textbook/light

[11] D. M. Bagnall and M. Boreland, "Photovoltaic technologies," *Energy Policy,* vol. 36, pp. 4390-4396, 2008.

[12] S. A. G. F. C. Krebs, "Production, Characterization and Stability of Organic Solar Cell Devices," PhD, Solar Energy Program, DTU, Roskilde: Risø National Laboratory for Sustainable Energy 2010.

[13] T. Liu, Y. Guo, Y. Yi, L. Huo, X. Xue, X. Sun*, et al.*, "Ternary organic solar cells based on two compatible nonfullerene acceptors with power conversion efficiency> 10%," *Advanced Materials,* vol. 28, pp. 10008-10015, 2016.

[14] W. Zhao, S. Li, H. Yao, S. Zhang, Y. Zhang, B. Yang*, et al.*, "Molecular Optimization Enables over 13% Efficiency in Organic Solar Cells," *Journal of the American Chemical Society,* 2017.

[15] A. Pochettino, "Sul comportamento foto-elettrico dell'antracene," *Acad. Lincei Rend,* vol. 15, p. 355, 1906.

[16] C. J. Mulligan, M. Wilson, G. Bryant, B. Vaughan, X. Zhou, W. J. Belcher*, et al.*, "A projection of commercial-scale organic photovoltaic module costs," *Solar Energy Materials and Solar Cells,* vol. 120, pp. 9-17, 2014.

[17] H. F. Dam. Available: http://plasticphotovoltaics.org/lc/lc-polymersolarcells/lc-how.html#fr1

[18] W. R. Cao and J. G. Xue, "Recent progress in organic photovoltaics: device architecture and optical design," *Energy & Environmental Science,* vol. 7, pp. 2123-2144, Jul 2014.

[19] M. C. Scharber and N. S. Sariciftci, "Efficiency of bulk-heterojunction organic solar cells," *Progress in Polymer Science,* vol. 38, pp. 1929-1940, Dec 2013.

[20] A. J. Heeger, "Semiconducting and metallic polymers: the fourth generation of polymeric materials (Nobel lecture)," *Angewandte Chemie International Edition,* vol. 40, pp. 2591-2611, 2001.

[21] R. Gaudiana, "Third-generation photovoltaic technology–the potential for low-cost solar energy conversion," ed: ACS Publications, 2010.

[22] W. Shockley and H. J. Queisser, "Detailed balance limit of efficiency of p-n junction solar cells," *Journal of applied physics,* vol. 32, pp. 510-519, 1961.

[23] BusinessHire. (2012). *CORRECTING and REPLACING Phillips 66, South China University of Technology, and Solarmer Energy Set a World Record in Solar Power Conversion Efficiency*. Available: http://www.businesswire.com/news/home/20120821005794/en/CORRECTING-REPLACING-Phillips-66-South-China-University

[24] NREL. (2017, 02/08/2017). *Best Research Cell Efficiencies* Available: https://www.nrel.gov/pv/assets/images/efficiency-chart.png

[25] R. Roesch, K.-R. Eberhardt, S. Engmann, G. Gobsch, and H. Hoppe, "Polymer solar cells with enhanced lifetime by improved electrode stability and sealing," *Solar Energy Materials and Solar Cells,* vol. 117, pp. 59-66, 2013.

[26] N. K. Elumalai and A. Uddin, "Open circuit voltage of organic solar cells: an in-depth review," *Energy & Environmental Science,* vol. 9, pp. 391-410, 2016.

[27] C. Deibel and V. Dyakonov, "Polymer–fullerene bulk heterojunction solar cells," *Reports on Progress in Physics,* vol. 73, p. 096401, 2010.

[28] Y. Lin and X. Zhan, "Non-fullerene acceptors for organic photovoltaics: an emerging horizon," *Materials Horizons,* vol. 1, pp. 470-488, 2014.

[29] Q. Wang, Y. Xie, F. Soltani-Kordshuli, and M. Eslamian, "Progress in emerging solution-processed thin film solar cells - Part I: Polymer solar cells," *Renewable & Sustainable Energy Reviews,* vol. 56, pp. 347-361, Apr 2016.

[30] C. K. Chiang, C. Fincher Jr, Y. W. Park, A. J. Heeger, H. Shirakawa, E. J. Louis*, et al.*, "Electrical conductivity in doped polyacetylene," *Physical review letters,* vol. 39, p. 1098, 1977.

[31] R. Balint, N. J. Cassidy, and S. H. Cartmell, "Conductive polymers: Towards a smart biomaterial for tissue engineering," *Acta Biomaterialia,* vol. 10, pp. 2341-2353, 2014/06/01/ 2014.

[32] J. Bredas, R. Chance, and R. Silbey, "Comparative theoretical study of the doping of conjugated polymers: polarons in polyacetylene and polyparaphenylene," *Physical Review B,* vol. 26, p. 5843, 1982.

[33] J. D. Stenger-Smith, "Intrinsically electrically conducting polymers. Synthesis, characterization, and their applications," *Progress in Polymer Science,* vol. 23, pp. 57-79, 1998.

[34] D. Fichou, "Structural order in conjugated oligothiophenes and its implications on opto-electronic devices," *Journal of Materials Chemistry,* vol. 10, pp. 571-588, 2000.

[35] C. E. Small, S. Chen, J. Subbiah, C. M. Amb, S.-W. Tsang, T.-H. Lai*, et al.*, "High-efficiency inverted dithienogermole-thienopyrrolodione-based polymer solar cells," *Nature Photonics,* vol. 6, pp. 115-120, 2012.

[36] Y. Sun, J. H. Seo, C. J. Takacs, J. Seifter, and A. J. Heeger, "Inverted polymer solar cells integrated with a low-temperature-annealed sol-gel-derived ZnO film as an electron transport layer," *Advanced Materials,* vol. 23, pp. 1679-1683, 2011.

[37] M. De Jong, L. Van Ijzendoorn, and M. De Voigt, "Stability of the interface between indium-tin-oxide and poly (3, 4-ethylenedioxythiophene)/poly (styrenesulfonate) in polymer light-emitting diodes," *Applied Physics Letters,* vol. 77, pp. 2255-2257, 2000.

[38] H. Hoppe and N. S. Sariciftci, "Organic solar cells: An overview," *Journal of Materials Research,* vol. 19, pp. 1924-1945, 2004/007/001 2004.

[39] (11-06-2017). Available: https://en.wikipedia.org/wiki/Organic_solar_cell

[40] M. D. McGehee and M. A. Topinka, "Solar cells: Pictures from the blended zone," *Nature materials,* vol. 5, pp. 675-676, 2006.

[41] J. Nelson, "Organic photovoltaic films," *Current Opinion in Solid State and Materials Science,* vol. 6, pp. 87-95, 2002.

[42] B. Weinberger, M. Akhtar, and S. Gau, "Polyacetylene photovoltaic devices," *Synthetic Metals,* vol. 4, pp. 187-197, 1982.

[43] S. Glenis, G. Tourillon, and F. Garnier, "Influence of the doping on the photovoltaic properties of thin films of poly-3-methylthiophene," *Thin Solid Films,* vol. 139, pp. 221-231, 1986.

[44] S. Karg, W. Riess, V. Dyakonov, and M. Schwoerer, "Electrical and optical characterization of poly (phenylene-vinylene) light emitting diodes," *Synthetic metals,* vol. 54, pp. 427-433, 1993.

[45] J. J. Halls and R. H. Friend, "Organic photovoltaic devices," *Clean electricity from photovoltaics,* pp. 377-432, 2001.

[46] N. Yeh and P. Yeh, "Organic solar cells: Their developments and potentials," *Renewable & Sustainable Energy Reviews,* vol. 21, pp. 421-431, May 2013.

[47] N. Sariciftci, D. Braun, C. Zhang, V. Srdanov, A. Heeger, G. Stucky*, et al.*, "Semiconducting polymer-buckminsterfullerene heterojunctions: Diodes, photodiodes, and photovoltaic cells," *Applied physics letters,* vol. 62, pp. 585-587, 1993.

[48] C. W. Tang, "Two-layer organic photovoltaic cell," *Applied Physics Letters,* vol. 48, pp. 183-185, 1986.

[49] P. Peumans and S. Forrest, "Very-high-efficiency double-heterostructure copper phthalocyanine/C 60 photovoltaic cells," *Applied Physics Letters,* vol. 79, pp. 126-128, 2001.

[50] P. Peumans and S. Forrest, "Erratum:" Very-high-efficiency double-heterostructure copper phthalocyanine/C60 photovoltaic cells"(Appl. Phys. Lett. 79, 126 (2001))," *Applied Physics Letters,* vol. 80, p. 338, 2002.

[51] M. Granström, K. Petritsch, A. Arias, A. Lux, M. Andersson, and R. Friend, "Laminated fabrication of polymeric photovoltaic diodes," *Nature,* vol. 395, pp. 257-260, 1998.

[52] L. Chen, D. Godovsky, O. Inganäs, J. C. Hummelen, R. Janssens, M. Svensson*, et al.*, "Polymer photovoltaic devices from stratified multilayers of donor–acceptor blends," *Advanced materials,* vol. 12, pp. 1367-1370, 2000.

[53] A. Loiudice, A. Rizzo, M. Biasiucci, and G. Gigli, "Bulk heterojunction versus diffused bilayer: the role of device geometry in solution p-doped polymer-based solar cells," *The journal of physical chemistry letters,* vol. 3, pp. 1908-1915, 2012.

[54] G. Yu, J. Gao, J. C. Hummelen, F. Wudl, and A. J. Heeger, "Polymer photovoltiac cells: Enhanced efficiencies via a network of internal donor-acceptor heterojunctions," *Science,* vol. 270, p. 1789, 1995.

[55] S. E. Shaheen, C. J. Brabec, N. S. Sariciftci, F. Padinger, T. Fromherz, and J. C. Hummelen, "2.5% efficient organic plastic solar cells," *Applied Physics Letters,* vol. 78, pp. 841-843, 2001.

[56] F. Padinger, R. S. Rittberger, and N. S. Sariciftci, "Effects of postproduction treatment on plastic solar cells," *Advanced Functional Materials,* vol. 13, pp. 85-88, 2003.

[57] J. Xue, B. P. Rand, S. Uchida, and S. R. Forrest, "Mixed donor-acceptor molecular heterojunctions for photovoltaic applications. II. Device performance," *Journal of Applied Physics,* vol. 98, p. 124903, 2005.

[58] M. A. Green, K. Emery, Y. Hishikawa, and W. Warta, "Solar cell efficiency tables (version 35)," *Progress in photovoltaics: Research and applications,* vol. 18, pp. 144-150, 2010.

[59] S. H. Park, A. Roy, S. Beaupré, S. Cho, N. Coates, J. S. Moon*, et al.*, "Bulk heterojunction solar cells with internal quantum efficiency approaching 100%," *Nature photonics,* vol. 3, pp. 297-302, 2009.

[60] J. Peet, J. Y. Kim, N. E. Coates, W. L. Ma, D. Moses, A. J. Heeger*, et al.*, "Efficiency enhancement in low-bandgap polymer solar cells by processing with alkane dithiols," *Nature materials,* vol. 6, pp. 497-500, 2007.

[61] H. Hoppe, N. Arnold, N. Sariciftci, and D. Meissner, "Modeling the optical absorption within conjugated polymer/fullerene-based bulk-heterojunction organic solar cells," *Solar energy materials and solar cells,* vol. 80, pp. 105-113, 2003.

[62] E. Lioudakis, A. Othonos, I. Alexandrou, and Y. Hayashi, "Optical properties of conjugated poly (3-hexylthiophene)/[6, 6]-phenyl C 61-butyric acid methyl ester composites," *Journal of Applied Physics,* vol. 102, p. 083104, 2007.

[63] S. Martin, D. Bradley, P. Lane, H. Mellor, and P. Burn, "Linear and nonlinear optical properties of the conjugated polymers PPV and MEH-PPV," *Physical Review B,* vol. 59, p. 15133, 1999.

[64] W. J. Beenken, "Excitons in conjugated polymers: Do we need a paradigma change?," *physica status solidi (a),* vol. 206, pp. 2750-2756, 2009.

[65] R. Österbacka, C. P. An, X. Jiang, and Z. V. Vardeny, "Two-dimensional electronic excitations in self-assembled conjugated polymer nanocrystals," *Science,* vol. 287, pp. 839-842, 2000.

[66] C. Kästner, K. Vandewal, D. A. M. Egbe, and H. Hoppe, "Revelation of interfacial energetics in organic multiheterojunctions," *Advanced Science,* vol. 4, 2017.

[67] D. Markov, C. Tanase, P. Blom, and J. Wildeman, "Simultaneous enhancement of charge transport and exciton diffusion in poly (p-phenylene vinylene) derivatives," *Physical Review B,* vol. 72, p. 045217, 2005.

[68] D. E. Markov, E. Amsterdam, P. W. Blom, A. B. Sieval, and J. C. Hummelen, "Accurate measurement of the exciton diffusion length in a conjugated polymer using a heterostructure with a side-chain cross-linked fullerene layer," *The Journal of Physical Chemistry A,* vol. 109, pp. 5266-5274, 2005.

[69] O. V. Mikhnenko, H. Azimi, M. Scharber, M. Morana, P. W. Blom, and M. A. Loi, "Exciton diffusion length in narrow bandgap polymers," *Energy & Environmental Science,* vol. 5, pp. 6960-6965, 2012.

[70] G. P. Smestad, F. C. Krebs, C. M. Lampert, C. G. Granqvist, K. Chopra, X. Mathew*, et al.*, "Reporting solar cell efficiencies in solar energy materials and solar cells," ed: Elsevier, 2008.

[71] N. S. Sariciftci, L. Smilowitz, A. J. Heeger, and F. Wudl, "Photoinduced electron transfer from a conducting polymer to buckminsterfullerene," *Science,* pp. 1474-1476, 1992.

[72] L. Onsager, "Initial Recombination of Ions," *Physical Review,* vol. 54, pp. 554-557, 10/15/ 1938.

[73] C. L. Braun, "Electric field assisted dissociation of charge transfer states as a mechanism of photocarrier production," *The Journal of chemical physics,* vol. 80, pp. 4157-4161, 1984.

[74] C. Deibel, T. Strobel, and V. Dyakonov, "Origin of the efficient polaron-pair dissociation in polymer-fullerene blends," *Physical review letters,* vol. 103, p. 036402, 2009.

[75] S. Holdcroft, "A photochemical study of poly (3-hexylthiophene)," *Macromolecules,* vol. 24, pp. 4834-4838, 1991.

[76] L. Y. Lu, T. Y. Zheng, Q. H. Wu, A. M. Schneider, D. L. Zhao, and L. P. Yu, "Recent Advances in Bulk Heterojunction Polymer Solar Cells," *Chemical Reviews,* vol. 115, pp. 12666-12731, Dec 2015.

[77] I. Riedel and V. Dyakonov, "Influence of electronic transport properties of polymer-fullerene blends on the performance of bulk heterojunction photovoltaic devices," *physica status solidi (a),* vol. 201, pp. 1332-1341, 2004.

[78] A. Kumar, S. Sista, and Y. Yang, "Dipole induced anomalous S-shape I-V curves in polymer solar cells," *Journal of Applied Physics,* vol. 105, p. 094512, 2009.

[79] V. Mihailetchi, P. Blom, J. Hummelen, and M. Rispens, "Cathode dependence of the open-circuit voltage of polymer: fullerene bulk heterojunction solar cells," *Journal of Applied Physics,* vol. 94, pp. 6849-6854, 2003.

[80] L. M. Chen, Z. Hong, G. Li, and Y. Yang, "Recent progress in polymer solar cells: manipulation of polymer: fullerene morphology and the formation of efficient inverted polymer solar cells," *Advanced Materials,* vol. 21, pp. 1434-1449, 2009.

[81] A. J. Moulé and K. Meerholz, "Morphology Control in Solution-Processed Bulk-Heterojunction Solar Cell Mixtures," *Advanced Functional Materials,* vol. 19, pp. 3028-3036, 2009.

[82] A. J. Heeger, "25th Anniversary Article: Bulk Heterojunction Solar Cells: Understanding the Mechanism of Operation," *Advanced Materials,* vol. 26, pp. 10-28, 2014.

[83] J. Liu, Y. Shi, and Y. Yang, "Solvation-induced morphology effects on the performance of polymer-based photovoltaic devices," *Advanced Functional Materials,* vol. 11, p. 420, 2001.

[84] S. J. Lou, J. M. Szarko, T. Xu, L. Yu, T. J. Marks, and L. X. Chen, "Effects of additives on the morphology of solution phase aggregates formed by active layer components of high-efficiency organic solar cells," *Journal of the American Chemical Society,* vol. 133, pp. 20661-20663, 2011.

[85] Y. Yang, Z.-G. Zhang, H. Bin, S. Chen, L. Gao, L. Xue*, et al.*, "Side-chain isomerization on an n-type organic semiconductor ITIC acceptor makes 11.77% high efficiency polymer solar cells," *Journal of the American Chemical Society,* vol. 138, pp. 15011-15018, 2016.

[86] D. A. M. Egbe, G. Adam, A. Pivrikas, A. M. Ramil, E. Birckner, V. Cimrova*, et al.*, "Improvement in carrier mobility and photovoltaic performance through random distribution of segments of linear and branched side chains," *Journal of Materials Chemistry,* vol. 20, pp. 9726-9734, 2010.

[87] Y. Lin, J. Wang, Z.-G. Zhang, H. Bai, Y. Li, D. Zhu*, et al.*, "An Electron Acceptor Challenging Fullerenes for Efficient Polymer Solar Cells," *Advanced Materials,* vol. 27, pp. 1170-1174, 2015.

[88] S. Lattante, "Electron and hole transport layers: their use in inverted bulk heterojunction polymer solar cells," *Electronics,* vol. 3, pp. 132-164, 2014.

[89] D. Yang, P. Fu, F. Zhang, N. Wang, J. Zhang, and C. Li, "High efficiency inverted polymer solar cells with room-temperature titanium oxide/polyethylenimine films as electron transport layers," *Journal of Materials Chemistry A,* vol. 2, pp. 17281-17285, 2014.

[90] M. Namazian, C. Y. Lin, and M. L. Coote, "Benchmark calculations of absolute reduction potential of ferricinium/ferrocene couple in nonaqueous solutions," *Journal of chemical theory and computation,* vol. 6, pp. 2721-2725, 2010.

[91] N. Zawacka. (17-07-2017). Available: http://plasticphotovoltaics.org/lc/characterization/lc-advanced-c/lc-elec-mea.html

[92] NREL. Available: http://rredc.nrel.gov/solar/spectra/am1.5/ASTMG173/ASTMG173.html

[93] U. Dasgupta, A. Bera, and A. J. Pal, "Band Diagram of Heterojunction Solar Cells through Scanning Tunneling Spectroscopy," *ACS Energy Letters,* vol. 2, pp. 582-591, 2017.

[94] B. P. Rand, D. P. Burk, and S. R. Forrest, "Offset energies at organic semiconductor heterojunctions and their influence on the open-circuit voltage of thin-film solar cells," *Physical Review B,* vol. 75, p. 115327, 2007.

[95] Z. Zheng, O. M. Awartani, B. Gautam, D. Liu, Y. Qin, W. Li*, et al.*, "Efficient Charge Transfer and Fine-Tuned Energy Level Alignment in a THF-Processed Fullerene-Free Organic Solar Cell with 11.3% Efficiency," *Advanced Materials,* vol. 29, 2017.

[96] F. C. Krebs, T. D. Nielsen, J. Fyenbo, M. Wadstrøm, and M. S. Pedersen, "Manufacture, integration and demonstration of polymer solar cells in a lamp for the "Lighting Africa" initiative," *Energy & Environmental Science,* vol. 3, pp. 512-525, 2010.

Appendix

A.1 Scan of films and devices fabricated from different material combinations

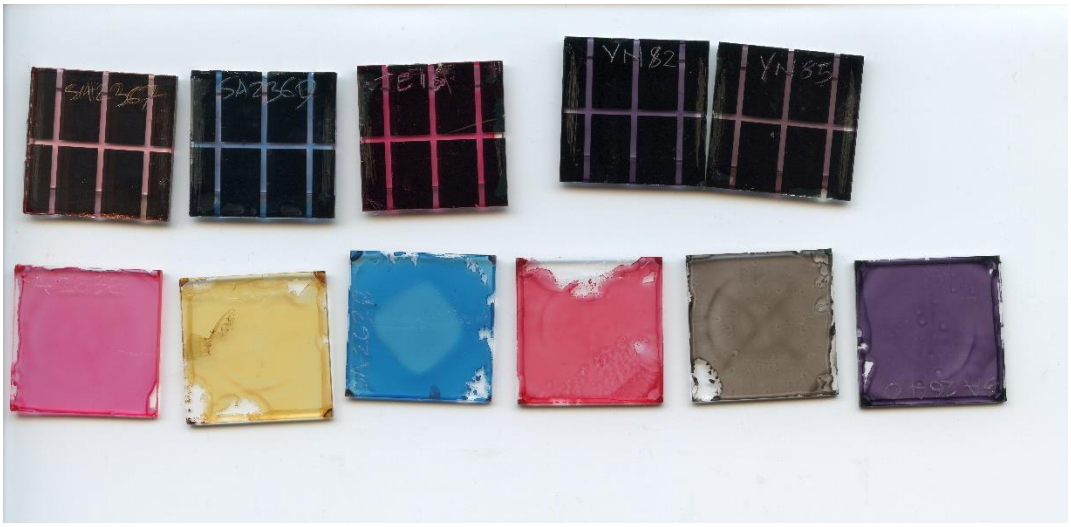

A 1 Film and cells spincoated with different active layers

A.2 Screenshot of Measurement Equipment and Interfaces

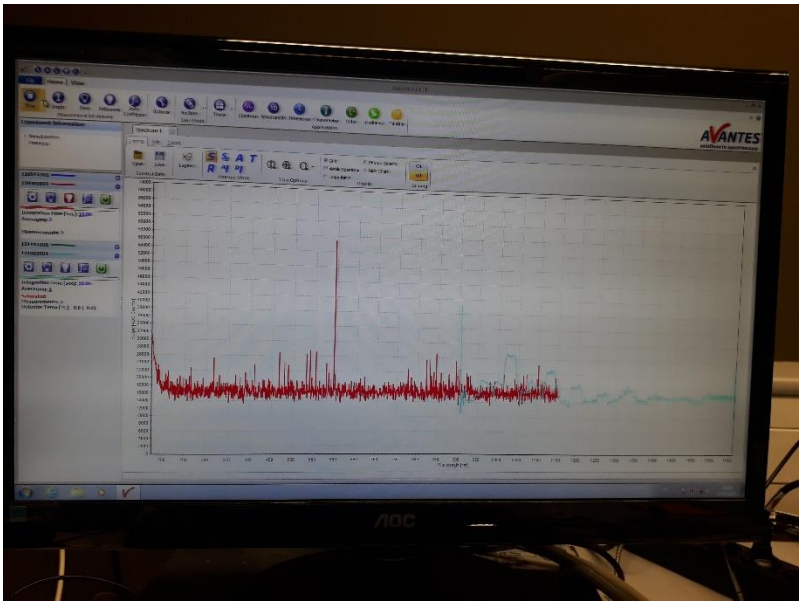

A 2: Avasoft Interface for UV-Vis and PL spectroscopy

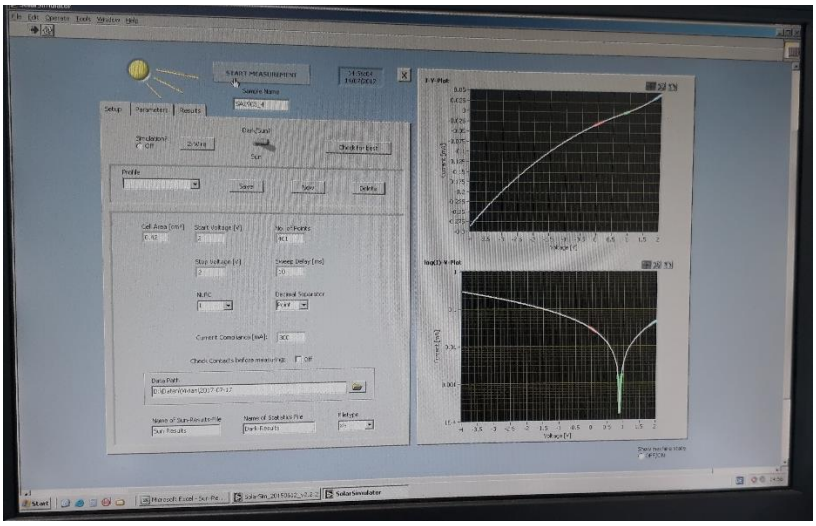

A 3: Solar simulator interface for device measurement under illumination

A 4: Device with four cells being characterized

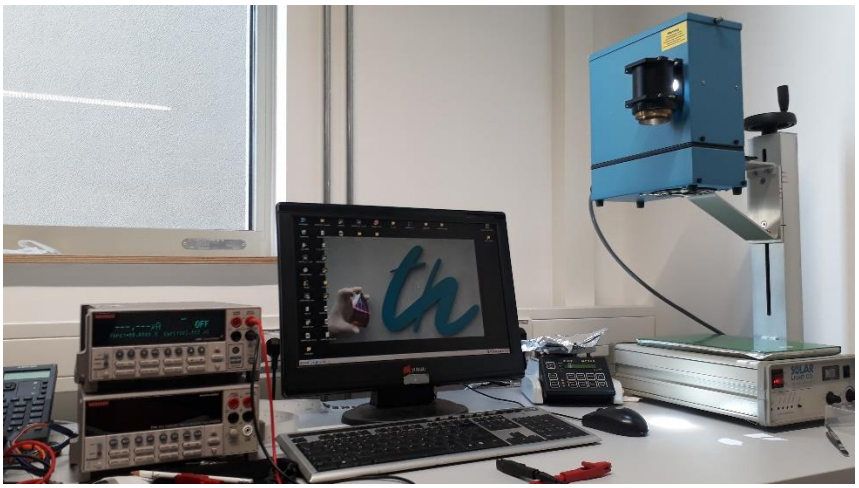

A 5 : Full setup for electrical characterization showing Keithley as Voltage source and the xenon lamp for illumination

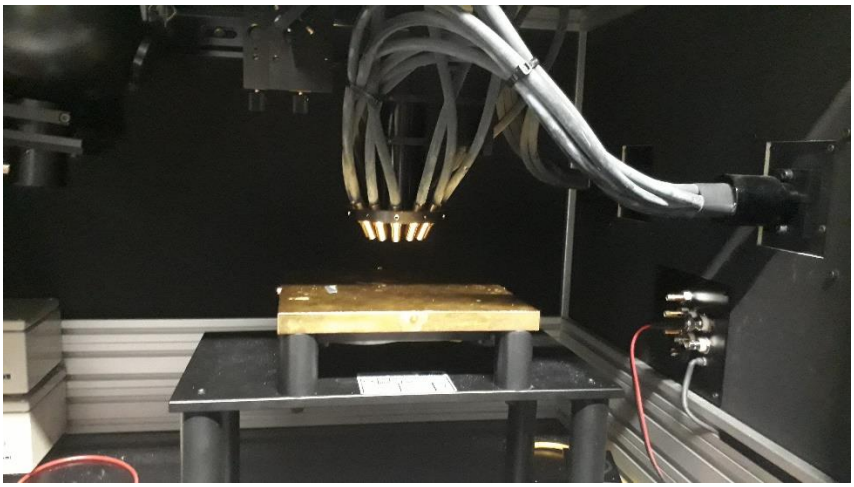

A 6: Setup for EQE measurement

A3 Optical Properties for reference material

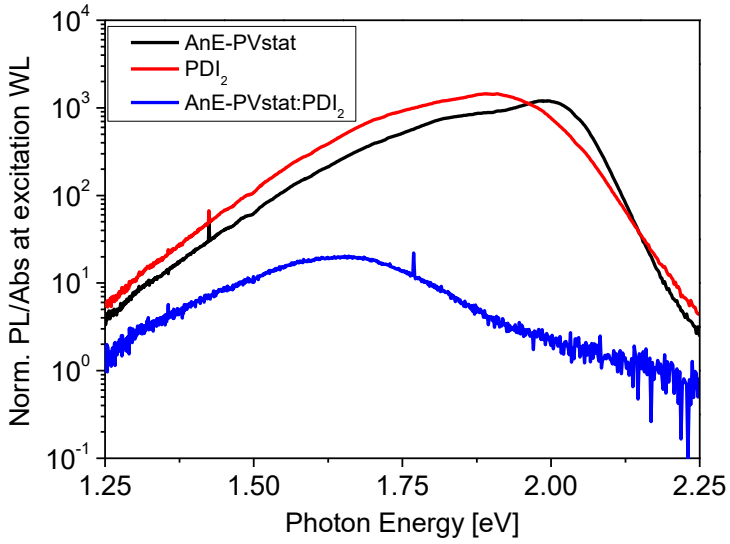

A 7: Photoluminescence spectra of PDI_2

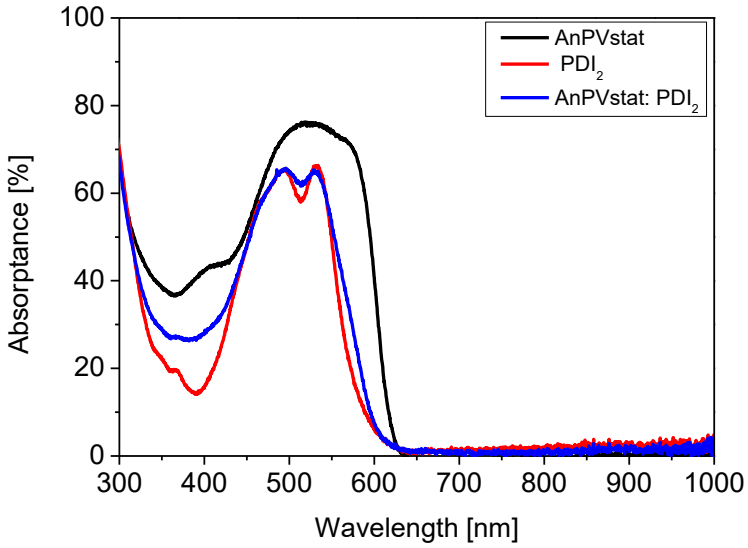

A 8: Absorption Spectra of PDI_2